Determining the Radon Emanation Coefficient for Soil Samples

by

Lebogang Phefo

A dissertation submitted for partial fulfillment of the requirements for the degree of Master of Science at the University of Zululand

Department of Physics and Engineering
University of Zululand
South Africa

Supervisors:

Prof. R. Lindsay
Department of Physics and Astronomy
University of the Western Cape

Prof. S.S Ntshangase
Department of Physics and Engineering
University of Zululand

Prof. R.T Newman
Department of Physics
Stellenbosch University

Abstract

Exposure to high concentrations of radon and radon decay products are known to increase lung cancer in humans. This study is in preparation for a national indoor radon survey to be conducted in South Africa. The aim of this study is to determine the radon emanation coefficient for soil samples collected in various areas in South Africa. The radon emanation coefficient is important for identifying areas with high radium concentrations which emanate radon which could lead to high levels of radon in houses. The areas of interest for this study include Paarl and Saldanha (having granite outcrops), Kloof and Boksburg mine dumps, Centurion, West Coast and Richards Bay Minerals where high radon levels are expected. The soil samples were collected and analysed in the laboratory. Both alpha and gamma spectrometry were used for determining the radium activity concentration of the soil samples and the radon released by the soil from which the radon emanation coefficient can be found. The samples were sealed for a period of 21 days to achieve secular equilibrium between radium and radon and then counted using a NaI(Tl) detector to measure the radium activity using a ^{214}Bi full-energy peak. The radon concentration was determined using an active radon monitor, the RAD7 which measures the alpha particles emitted from the radon progenies, ^{218}Po and ^{214}Po. The values obtained for the radium activity concentration varied in the range of 9.206×10^3, 94 - 1146, 339 - 368, 64 - 147, 72, 18 - 34 and 11 $Bq.kg^{-1}$ for West Coast, Boksburg, Kloof, Paarl, Richards Bay Minerals, Saldanha and Centurion samples, respectively. The radon concentration values built up in the accumulation chamber (of 10 litres) to values of 233, 175 - 596, 225 - 352, 218 - 223, 358, 61 - 99, 58 $Bq.m^{-3}$ in West Coast, Boksburg, Kloof, Paarl, Richards Bay Minerals, Saldanha, and Centurion for soil samples having the mass of about 0.256 kg, respectively. Finally, the emanation coefficient was determined as the fraction of the radon atoms created that is exhaled into the air and the radium activity. The values of the emanation coefficient obtained in this study for sample mass of 0.256 kg ranges from, 0.073 - 0.146, 0.063 - 0.313, 0.214 - 0.541, 0.276 - 0.847, 0.812, 0.765 and 0.004, in Kloof, Boksburg, Paarl, Saldanha, Centurion, Richards Bay Minerals and West Coast, respectively. The radon emanation coefficient for sample mass of 0.512 kg are in the ranges from 0.092 - 0.108, 0.139 - 0.326, 0.171 - 0.572, 0.169 - 0.774, 0.188, 0.003, in Kloof, Boksburg, Paarl, Saldanha, Centurion, Richards Bay Minerals and West Coast, respectively. The radon emanation for the final sample mass to be investigated ranges from 0.089 - 0.113, 0.139 - 0.275, 0.245 - 0.373, 0.296 - 0.738, 0.686, 0.157, 0.003, Kloof, Boksburg, Paarl, Saldanha, Centurion, Richards Bay Minerals and West Coast, respectively. These values of the emanation coefficient are in line with wide ranging values of 0.01 - 0.8 reported in the UNSCEAR 2000 report. These values will help to choose the distribution of houses that should be measured in the planned survey of radon in houses.

Declaration

I, Lebogang Phefo the undersigned, hereby declare that the work contained in this thesis is my own original work and that I have not previously in its entirety or in part submitted it at any university for a degree.

Signed: _____

Date: _____

Acknowledgements

I would like to acknowledge the Father of lights (God), who has been the source of peace, strength and hope, who has carried me throughout this project.

To the following people and institutions I will forever be indebted to you. It has been a great privilege for me to have worked with you in this project.

- To the National Research Foundation (NRF), for funding this work through the MANUS/MATSCI- a joint programme between the University of Zululand, University of the Western Cape and iThemba LABS and also the National Nuclear Regulator (NNR) for their contributions in this project. I am grateful that through this fundings I was able to realize my dreams.
- My project supervisors: Prof Robert Lindsay, Prof Sifiso Senzo Ntshangase and Prof Richard Thomas Newman, for their guidance and technical support, as well as financial contribution and willingness to assist to complete this project.
- The Department of Physics and Astronomy at the University of the Western Cape, for the kind support and assistance throughout the course of the study.
- To my collegues, Elmughera Elhag, Dr Joash Ongori for always helping me regards to my project.
- My mother, Basetsana Phefo and my siblings and all my friends for their love, encouragement and prayers throughout.

Contents

List of Figures

List of Tables

Chapter 1

Introduction

1.1 Discovery of radon

In this chapter a brief introduction is given on the theory of radioactivity and the discovery of radon, an overview on the formation, migration and emanation of radon is presented.

The earth has been radioactive from formation due to the presence of primordal radionuclides like uranium (^{238}U), thorium (^{232}Th), and potassium (^{40}K) with half-lives of 4.5×10^9, 14×10^9 and 1.3×10^9 years, respectively in the environment [1]. The radiation generated from these radionuclides forms part of the terrestrial radiation sources. Other radiation sources are from space and are called cosmic or cosmogenic radiation and man-made radiation which includes nuclear reactors and nuclear applications in medicine. Due to all these radiation sources human beings have and will continue being irradiated by these sources. The big question is how can we reduce the effects of these radiation sources to man-kind, hence the importance of research on radioactivity measurements and measures of counteracting their health implications. In the human environment, these radionuclides together with their decay products or progenies are present. In the decay chain of uranium (^{238}U), radium (^{226}Ra) is formed which is the immediate parent of radon (^{222}Rn). Radium was discovered by Marie Sklodowaska Curie in 1898. Two years later, in 1900, two isotopes of radon were discovered, thoron (^{220}Rn) by R.B Owens and E. Rutherford, and radon by Friedrich Ernst Dorn and he called it 'radium emanation'. It was later identified as radon (^{222}Rn) worldwide [19].

The National Nuclear Regulator (NNR) has decided that a study should be performed to measure radon in houses in South Africa. This is a huge undertaking and a study is underway to come up with an affordable strategy. This study forms part of the national indoor radon survey as it focuses on determining the radon emanation coefficient of the soil since studies prove that the soil is one of the main sources of radon indoors [14],[62]. Several aspects play a role in how the radon gets drawn indoors such as, transportation, emanation and exhalation into the atmosphere. Studies suggests that at least 80% of radon released into the atmosphere comes from the top layers of the ground [46], hence the radon emanation plays an important role in the radon levels found in closed structures.

1.1.1 Physical and Chemical Properties of radon

Radon (^{222}Rn) is a gas at room temperature, it does not have a colour, taste and odour. It is chemically unreactive and can travel a long distance without mixing with other substances. It has atomic mass of 222, 86 protons and 136 neutrons. It decays by emitting a helium nucleus (2 protons and 2 neutrons) to form radioactive progenies. Its atomic symbol is Rn and it has a

density of 9.73 g/L (at STP) which is 7.5 times that of air. Radon has a boiling point of -61.7 °C and a melting point of -71 °C. It has three isotopes that occur naturally, radon (^{222}Rn), thoron (^{220}Rn) and actinon (^{219}Rn) with half-lives of 3.82 days, 55.6 seconds and 3.4 seconds, respectively [15]. Thoron is produced by radium (^{224}Ra) in the decay chain of thorium (^{232}Th), whereas, actinon is produced by radium (^{223}Ra) in the decay chain of uranium (^{235}U) [19]. The short half-life of ^{219}Rn and the low abundance of its parent makes its contribution negligible in measurements. The entrance of ^{222}Rn to the environment is much more than that of ^{220}Rn, therefore ^{220}Rn and its progenies are also neglected in this study [1] .

1.1.2 Health implications of radon decay products

Radon gas contributes about 50% to the background radiation exposure to the human population [67]. It behaves like an indoor air pollutant as it is hazardous to human beings, people spend about 90% of their time in confined structures e.g. homes and workplaces. Radon predominantly exists with its short-lived metal progenies (^{218}Po, ^{214}Pb, ^{214}Bi, and ^{214}Po) in the air and builds up to high levels in confined structures like homes and underground mines. The radon progenies are metal solids that attach to dust or smoke particles in the air. During inhalation of these progenies they can be deposited into the lungs and can damage the cells in the lungs due to alpha decay resulting in lung cancer. A high mortality in underground metal mine workers due to respiratory problems in 1500s was observed and that led to intense research on finding the cause. It was only in the 1960s that a clear link between radon and its decay products were observed to be the cause of lung cancer in underground uranium miners [38]. Futhermore, the observations from laboratory animals exposed to a uranium source and dust with radon decay products confirms the above findings [20]. Radon has been classified as the second leading cause of human lung cancer after cigarette smoking [48],[15].

1.1.3 Uses of radon

Changes in the radon levels have been studied as a pre-cursor to predict earthquakes [50] and volcanic eruptions, in underground mines and wells [69]. Monitoring of the radon gas levels is also useful in uranium exploration [65]. Its inertness makes it useful as a geophysical tracer for identifying buried faults and geological structures [71]. Radon can also be used in predicting the existence of petroleum and natural gas. Changes in radon levels is also used as an indicator for the presence of underground water. Measuring radon activities in soil gas and ground-water has been used to map faults and to characterize geothermal sources [19].

1.1.4 Different techniques for measuring radon

There are two common techniques of measuring radon concentration, (i) active or instantaneous and (ii) passive or time-integrated methods. The active mode of measuring radon requires electrical power and the measuring period of this technique is short. The latter do not use electrical power and the timescale of this type of measurement is in the order of weeks to months. Below are examples of passive techniques for measuring radon:

- Nuclear track detectors - uses a film material such as cellulose nitrate (LR-115 II), polycarbonate or allyl diglycol carbonate (CR 39). Here the alpha particles strike the film leaving microscopic tracks. The film is then etched using an alkaline solution and counted using a microscope. This type of detector has low sensitivity at short duration measurements and is better suited for soil gas radon measurements than for soil flux density measurements [29].

- Electret ion chambers - diffusion of radon gas into the chamber causes ionization of the air when radon decays thus reducing the surface voltage of the electrically charged teflon disc. The teflon disc acts as both a source of an electrostatic field and as a sensor. The electret reader is used to measure the voltages of the electret before and after exposure to determine the radon concentration. The exposure duration of this detector is in the range of days to months. One problem of this type of detector is that background gamma radiation also causes a drop in the voltage which requires a correction since the main signal of radon comes from alpha particles [29].

- Activated charcoal detectors - the charcoal absorbs the radon and the period of exposure is in the range of hours to few days. After exposure, the radon concentration is determined by gamma spectroscopy or liquid scintillation measurements that detects the radon progeny. A shortcoming of using this detector is that it is not suitable for wet or humid conditions and they can be used for short term measurements only [29].

Examples of active techniques for measuring radon:

- Solid state detectors - are made of semiconductor material that converts the alpha radiation to an electrical signal. They use a filter to prevent the radon progenies in the air from entering into the detector. This type of detector allows for the discrimination between the alpha particles from radon and thoron progenies. The disadvantage of this detector is using electrical power and its high cost. An example is the RAD7 radon monitor manufactured by Durridge company [29].

- A Lucas or scintillation cell is a continuous real time radon monitor. It detects alpha particles from radium and thoron as well [37].

1.1.5 Sources and transport of radon

Uranium is found in all rocks in trace amounts 1-3 ppm (parts per million), where 1ppm U is equivalent to 12.4 $Bq.kg^{-1}$ of ^{226}Ra, and it is a source of radon. The soil is formed from rocks through chemical and mechanical processes, hence the soils will also contain small amounts (1-3 ppm) of uranium. Radium is found in phosphate rocks, schist, gneiss and limestone and in well water and natural gas [59]. Various rock types have different contents of radionuclides (see Table 1.1).

Table 1.1: Typical contents of radionuclides in various rock types [21], [67].

Rock type	Uranium ($Bq.kg^{-1}$)	Thorium ($Bq.kg^{-1}$)	Potassium ($Bq.kg^{-1}$)
Granite	62	73	1176
Basalt	7	12	248
Shale	62	49	836
Sandstone	12	8	186
Limestone	22	7	93
Beach sand	37	24	93

From Table 1.1: Granite and shale rocks have high content of these three radionuclides, hence it can be assumed that the soil derived from these types of rock will have high content of the same radionuclides. Uranium being the parent of radium implies that its activity is the

same as in radium assuming a state of secular equilibrium. Hence, houses that are build on soil that has high contents of these radionuclides may have much higher indoor radon levels than usual [21].

1.1.6 The Transport of radon in a porous medium

Radon can be transported to the soil surface via two mechanism namely diffusion and advection. Diffusion is a transport mechanism due to the concentration differences in radon. Diffusion of radon is only dominant over short distances in the porous medium with a diffusion length of about a meter for dry soil with normal porosity [55]. Diffusion obeys Fick's law:

$$f = -D_M \nabla C \tag{1.1}$$

where
f is the radon flux density ($Bq.m^{-2}s^{-1}$);
D_M is the molecular diffusion coefficient ($m^2.s^{-1}$);
and ∇C is the gradient of radon activity concentration ($Bq.m^{-4}$)
Advection or convection is a transport mechanism caused by the flow of air containing radon, mainly due to pressure differentials. Advection is the dominant transport mechanism of radon over long distances that can exceed 100 meters [39]. Radon transport entry to houses is largely controlled by advection through cracks or gaps in the substructure. Advection obeys Darcy's law:

$$\vec{\nu} = -\frac{k}{\mu_a}\vec{\nabla} P_a \tag{1.2}$$

where
$\vec{\nu}$ = fluid flow per unit cross section ($m^3.m^{-2}s^{-1}$)
k = intrinsic permeability of the soil (m^2)
μ_a = dynamic viscosity of air ($Pa.s$)
P_a = air pressure (Pa) [63].

Transport of radon in a porous medium via advection and diffusion before it is exhaled from the medium which is soil in this study (see Figure 1.1).

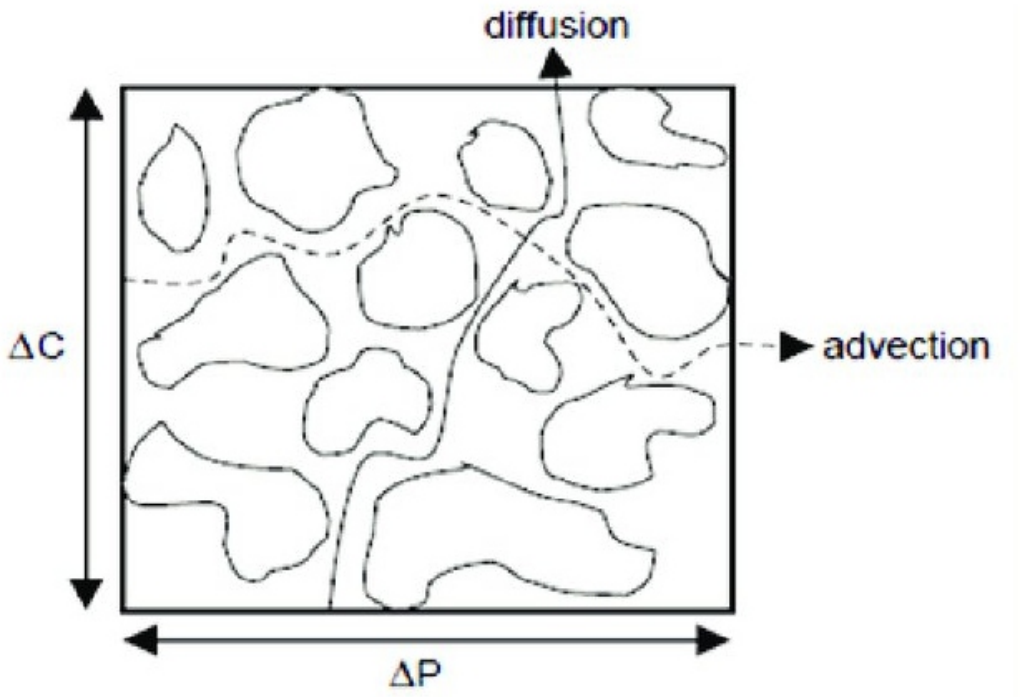

Figure 1.1: Radon transport in a porous medium by advection and diffusion [63].

The naturally occurring radon isotope (^{222}Rn) is formed by the alpha decay of uranium (^{238}U), as shown in Figure 1.2.

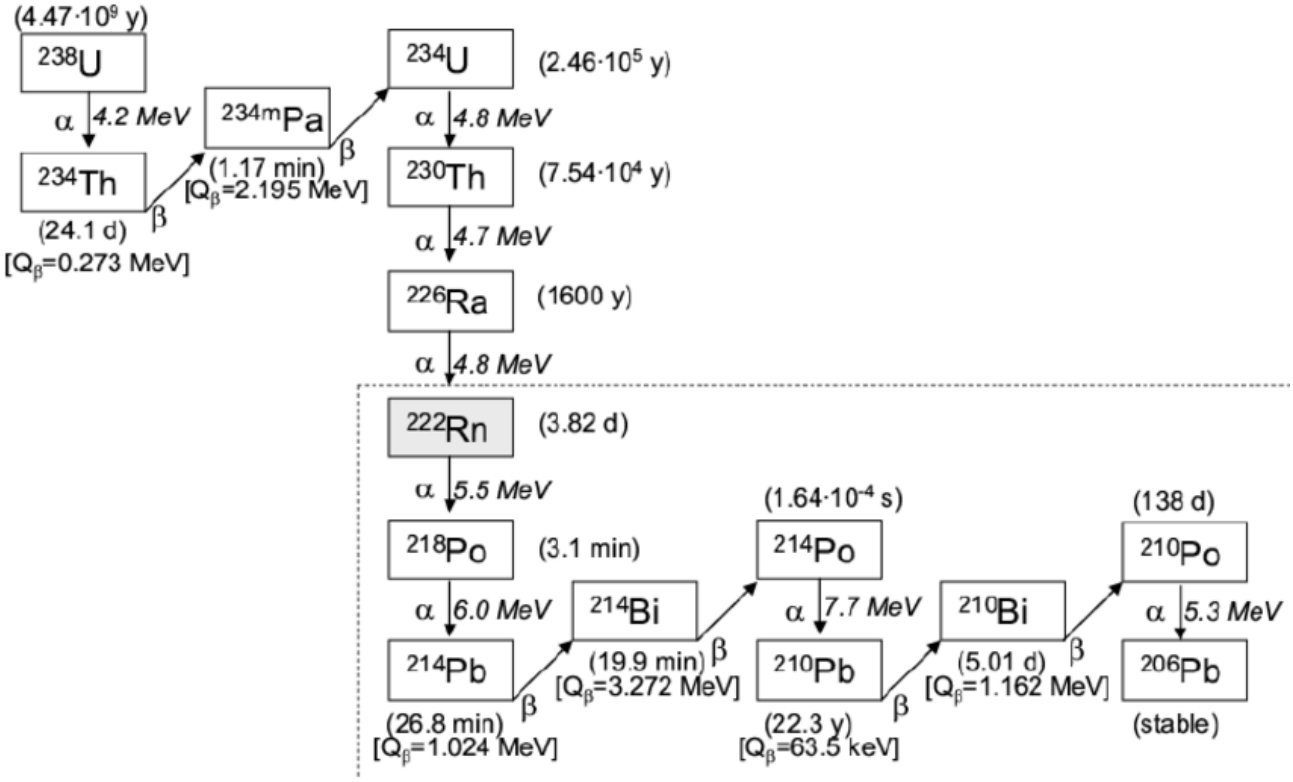

Figure 1.2: The decay chain of uranium [4]. The half-life and energies of the alpha and beta end point energies are indicated.

In the decay chain of uranium (^{238}U) that contains fourteen isotopes, radium (^{226}Ra), a solid is formed and is the immediate parent of radon (^{222}Rn). When a radium atom decays, it releases a radon atom having a recoil energy of 86 keV and an alpha particle having energy of 5.49 MeV moving in the opposite direction by the conservation of momentum. Not all the created radon escapes from the grains to the pore spaces, only a fraction escapes known as the radon emanation coefficient or fraction. Factors like the creation place of radon in the solid grain and the direction in which the radon recoils greatly influences the emanation coefficient [29]. Figure 1.3, shows the radon emanation process in the solid grains. The points (A, B, E and F) shows areas where the radon emanation has occurred i.e points that contribute to the radon emanation coefficient. The radon atoms points (A, B, E and F) are located within the recoiling range and their direction is facing outward from the grains which favours radon escape. The other points (C, D and G) shows that no radon emanation has occurred and do not contribute to the radon emanation coefficient since their final point is inside a grain.

The radon atom that gets embedded into adjacent grains can still emanate to the pore spaces due to the passage caused by the radiation damage. This can happen if it was embedded on the surface or edge of the grain contributing to the increase in radon emanation coefficient. The radon atoms that are embedded within the grains do not contribute to the radon emanation coefficient since they do not make it to the pore space and they are not within the recoil range [30]. Radon atoms that emanate from solid grains can escape to the pore space filled with air, water or can escape into adjacent grains [54]. If the pore space is filled with air, the radon atom can easily move from the creation site and into another grain and never contribute to the emanation coefficient. In the case where the pore space is filled with water, the radon atom will usually be stopped in the pore space due to the fact that water has a much higher stopping power than air and thereby will contribute to the radon emanation coefficient. Lastly, if the

radon atom cannot diffuse outside the host grain, the recoil will be the main influencing factor for the radon to escape from the solid grains. Radon emanation coefficients can have values between 0 and 1. When there is no radon escaping from the host material it is 0 and when all the radon that is created escapes to the pore spaces it is 1 [8]. The emanation coefficient is dimensionless and can be given as a fraction or percentage [65]. Figure 1.3 represents the radon emanation process in soil grains.

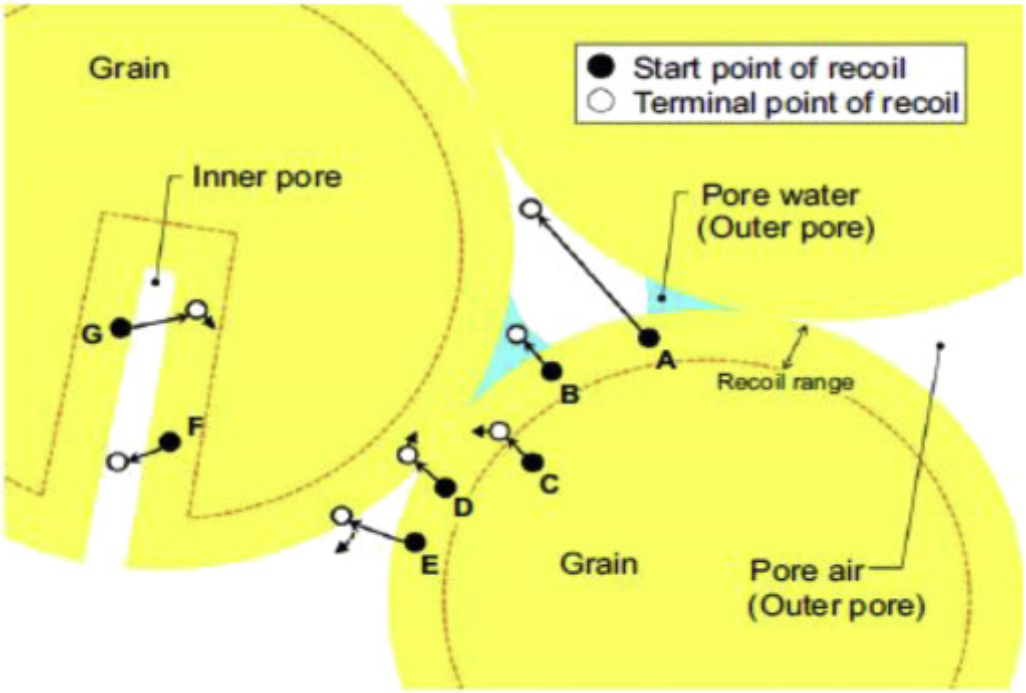

Figure 1.3: Schematic of the radon emanation process [29].

The radon atoms that do escape to the pore spaces are the ones that can be carried to the ground surface by processes like diffusion and advection. It is not always the case that the radon in the pore spaces gets exhaled since this is dependent on the shape (e.g. grain size) and the porosity of the soil. Radon has small diffusion coefficients in solids of $10^{-31} - 10^{-69}\ m^2.s^{-1}$ which is equivalent to a diffusion length of $10^{-13} - 10^{-32}\ m$ [44], [54]. The diffusion length of radon in fine sand is about 166 cm and about 190 cm for gravel. For water saturated clay samples the diffusion length is only about 0.87 cm [61]. The recoil energy is the energy that is released during the decay of radium which can drive the newly created radon a distance of 40 nm from the site of generation in solid materials [54].

The density and the construction of the material determines how long the radon can travel in the grain [72]. In quartz, the recoil range the radon atoms can travel is about 34 nm, in water about 77 nm and for air about 53 μm [29]. These values were calculated using SRIM-2006 code [54], [42]. Other factors like temperature, moisture content, pore size, grain size etc., influences the radon emanation coefficient. Many models have been used to explain the role of environmental conditions on the emanation [6], [9]. Only the radon atoms generated at the edges of the solid grains will escape into the pore space. The radon available in the pore space has a high chance of escaping to the ground surface, hence this study focuses on measuring the radon concentration in the pore spaces [7].

1.1.7 Radioactive decay processes

Radioactivity was accidentally discovered by Henri Becquerel in 1896 when he was testing for the phosphorecence of uranium salts. Radioactive decay is a spontaneous process that radionuclides undergo via the emission of particles like alpha, beta and gamma rays. During a radioactive decay not all the particles are released at once. The radioactive decay process is statistical in nature and hence it is not possible to predict when a specific atom will decay to form another. The activity of a radioactive sample having N nuclei decays proportionally to the decay constant.

$$A = \lambda N \tag{1.3}$$

The average number dN that will disintegrate in a short time dt is proportional to the number of atoms N present, that is:

$$\frac{dN}{dt} = -\lambda N \tag{1.4}$$

where λ is the decay constant of a specific radioactive species. Equation 1.4 can be integrated to give the solution called the exponential law of radioactive decay given below:

$$N(t) = N_0 e^{-\lambda t} \tag{1.5}$$

where N_0 is the original number of nuclei present at time t = 0. The above number of nuclei will slowly decay in some cases and faster in other species, but there will be a statistical time ($t_{1/2}$) after which half of the number of nuclei would have decayed. To get $t_{1/2}$, $N = N_0/2$ is substituted in equation 1.5 to give:

$$t_{1/2} = \frac{ln2}{\lambda} \tag{1.6}$$

which is called the half-life of a species. The activity of a radioactive sample is expressed in Becquerel (Bq), which is the number of decays per second [63], [43].

1.1.8 Types of Ionizing radiation

Alpha Particles

These particles are helium nuclei having two protons and two neutrons. During radioactive decay, mono-energetic alpha particles are produced e.g. $^{222}Rn \rightarrow {}^{218}Po + \alpha$. Alpha particles have doubly positive charge and high mass, they move slowly in matter dissipating all their energy in a short distance, resulting in dense ionization. Outside of the body, alpha radiation poses little health hazard but inside the body it can damage a lot of tissues when it hits living cells.

Beta Particles

These are high energy electrons of either positive or negative charge emitted from the nucleus of the atom. Unlike alpha particles, they travel larger distances in air and they move deeper into matter.

Neutrons

These have no charge and have almost the same mass as the protons and they are constituents of the nucleus of an atom. They are produced in nature from cosmic interaction with the atmosphere by collisions of high energy primary or secondary charged particles. They can also be produced in nuclear reactors and particle accelerators. Neutrons are classified into different types based on their energies: slow or thermal neutrons with energies in the order of electron volts (eV) and fast neutrons with energy in the order of mega electron volts (MeV).

Electromagnetic radiation

Gamma-rays and X-rays are high-energy photons. Gamma-rays are often released during alpha or beta decay from an atomic nucleus. X-rays are similar to gamma-rays except that they are produced when an orbital electron changes its energy level in the atom. The distances in which radiation can travel before penetrating a material is shown in Figure 1.4.

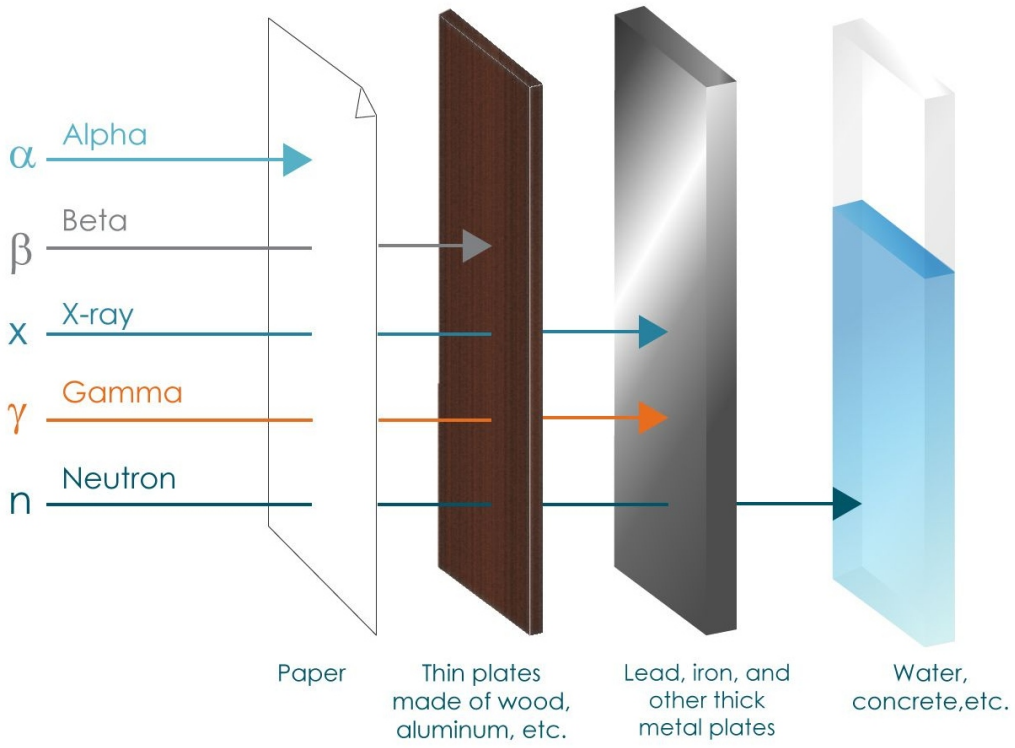

Figure 1.4: Schematic of the different radiations and penetration [66].

1.1.9 The measurement of gamma-rays

The measurement of gamma-rays depend on three ways in which they interact with matter:

- Photoelectric effect is a process whereby a photon is completely absorbed by a bound atomic electron (usually K electron) and lose all its energy to the ejected photoelectron. This gamma-ray interaction is dominant for low energy gamma-rays and for X-rays.
- Compton scattering is a process whereby a gamma-ray is incident on a weakly bound electron (outer electron) and transfers some of its energy to the electron. The ejected

electron and the scattered gamma-ray are released after interaction. This interaction dominates at intermediate energies between photoelectric effect and pair production.

- Pair production process occurs at energies larger than twice the rest mass of the electron at 1.022 MeV in the vicinity of the nucleus, where a gamma-ray creates an electron and a positron pair [45]. Figure 1.5 shows the schematic of the three main gamma-ray interactions.

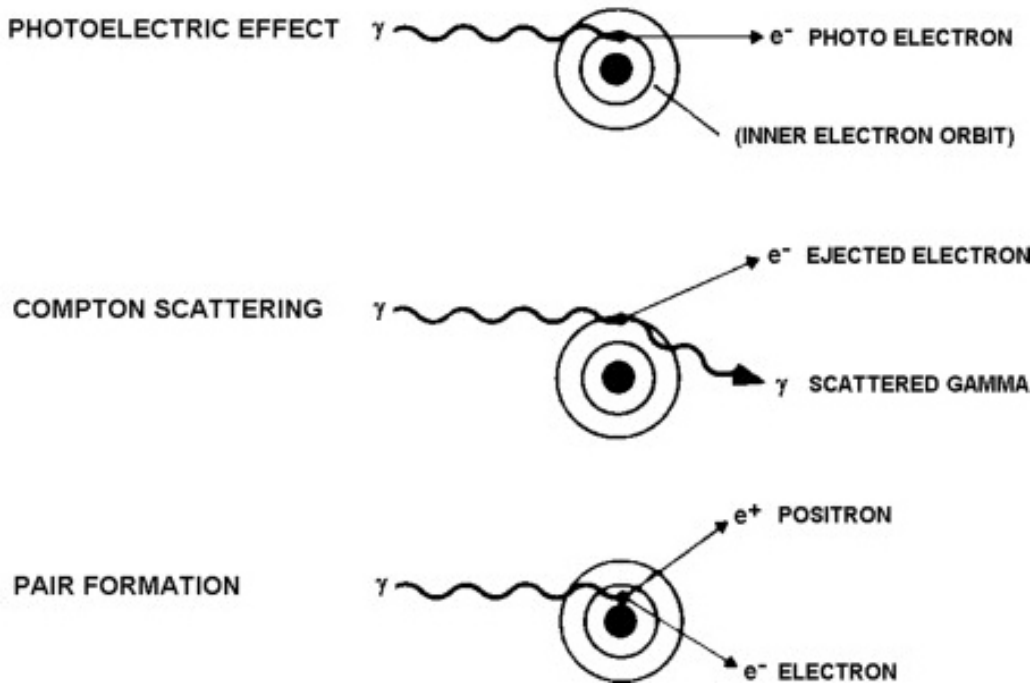

Figure 1.5: Schematic of the gamma-ray interactions with matter [13].

Chapter 2

Literature Review

2.1 Review of radon emanation studies

In this chapter, an overview on the literature is presented and in this study the focus will be on the measurement of the radon emanation coefficient from soil samples in South Africa. Some international and local studies where the emanation coefficient has been measured are discussed below. The type of detectors used are also presented in this section.

2.1.1 Rn-bubbler and Pylon AB-5 detector

A study was conducted by Greeman et al.,1996 [23] to measure the emanation coefficient of ^{222}Rn from 68 soil samples collected at 12 various places in the eastern U.S.A. The samples were extracted at a depth of 1.5 - 3.5 m at each place and sieved through a 2 mm mesh and only fine particles were used in the study. An improved technique of Rn-bubbler was used for determining the ^{226}Ra concentration. In a container, one sample that was not dried was placed together with a flask with water for a month and air was allowed to circulate through while the flask was intensely agitated in order to determine the radon concentration. The closed system was connected to an alpha scintillation cell for 10 minutes for the air to circulate. Radon was then allowed to reach equilibrium with its progenies. After six hours, the scintillation cell was counted on a Pylon AB-5 radon detector. The average values of the emanation coefficients over soil profiles ranged from 0.15 - 0.25. The value of the emanation coefficient was 0.22 for the silt-clay sample [22].

2.1.2 CR-39 detector

In the study by Abumurad et al.,1997 [1] seven sampling sites in Jordan were selected and soil samples extracted from five holes in each site. The holes were dug at depths of 20 - 100 cm at intervals of 20 cm. The holes where 1 meter apart. Alpha particles were detected using CR-39 Solid State Nuclear Track Detectors (SSNTDs) which can be exposed for a few weeks or more and only two were placed in each hole. After 15 days of measurement the dosimeters were gathered and etched using 6 N KOH at 70 $^{\circ}C$ for 8.5 hours and the tracks counted using an optical microscope. The study confirmed that the radon levels increases as the depth increased. The grain sizes were determined by crushing the rock samples, drying and sieving them. At a depth of 100 cm high radon levels of about 40 $kBq.m^{-3}$ were obtained in one site and another site gave a low value of 1.6 $kBq.m^{-3}$ at the same depth. A high emanation coefficient was reported from the soil samples enriched with radium which also showed high radon levels in the soil gas [1].

2.1.3 HPGe detector and Lucas Cell

An experiment by Holy et al.,1998 [27] was conducted to measure the radon emanation coefficient from two sandy soil samples in the Slovak Republic. The study also investigated the role of moisture content on the radon emanation coefficient. One sample was made of the sandy clay which was taken from a depth of 10 cm and the other sample made of sandy loam was taken from a depth of 120 cm in the ground. The samples were sieved and then oven dried at 105 $^{\circ}C$ for a few hours after which their grain sizes were determined. The samples were then sealed in Marinelli beakers and their ^{226}Ra activity concentration was determined after secular equilibrium between ^{226}Ra and ^{222}Rn was reached, using an HPGe detector. The full-energy peaks of ^{214}Pb (352 keV) and ^{214}Bi (609 keV) were used for determining the ^{226}Ra activity concentration. The samples were placed in a chamber that was sealed for 15 - 20 hours together with activated charcoal detectors and then moved into the scintillation counter (Lucas cell) for measuring the radon concentration. The thickness of the soil samples was made to be very small in relation to the diffusion length. Then the emanation coefficient (f) was calculated using the following equation:

$$f = \frac{E}{\lambda M A_{Ra}} \tag{2.1}$$

where E is the radon exhalation rate from the sample ($Bq.s^{-1}$), the decay constant of ^{222}Rn (s^{-1}) is given by λ, A_{Ra} is the ^{226}Ra activity concentration of the sample ($Bq.kg^{-1}$) and M is the dry mass of the sample in kg. The emanation coefficient was enhanced by the increase in the water content of the soil until a saturation point was reached. The sandy loam contained grains larger than 0.50 mm and it gave a low value of the emanation coefficient while the sandy clay is made up of grain sizes less than 0.25 mm which resulted in a high value of the emanation coefficient [27].

2.1.4 Electrostatic collector

An experiment by De Martino et al.,1998 [17] was conducted to measure the radon emanation coefficient and exhalation rate of soil samples. A silicon detector connected to an electrostatic collector was used in the experiment. The electrostatic collector was used for alpha particle detection to measure the concentration of ^{222}Rn and ^{220}Rn in the soil samples. Moreover, gamma spectroscopy using an HPGe (20 % efficiency and resolution of 1.9 keV at 1.33 MeV) detector was used to determine the ^{226}Ra and ^{232}Th activities using the full-energy peaks of ^{214}Pb and ^{214}Bi at 352 and 609 keV. The method of using electrostatic instrument was initiated by Keller et al.,1982 [17] for measuring radon levels indoors, outdoors and in the soil gas.

2.1.5 Kodak LR 115-II

An experiment by Baixeras et al.,2001 [5] was performed to measure the emanation coefficient of radon in the soil samples in Sweden (Lund region) and in Spain (Barcelona region). The soil samples were placed in plastic containers together with a Kodak LR 115-II film to measure the radon concentration. The container was placed inside a plastic bag that was sealed and stored for a period of 15 and 23 days. The activity concentration of ^{232}Th and ^{238}U was determined using gamma spectroscopy. The emanation coefficient was then measured from the fraction $\frac{C_{Rn}}{C_U}$ where C_{Rn} is the radon concentration in the container and C_U is the uranium concentration of the soil sample. The results gave a low radon emanation coefficient for sand even though it was richer in uranium than clay. Another sample made of alum shale had a high uranium content and had bigger grain size that resulted in a low emanation coefficient. The effect of grain size on the emanation coefficient explains why some houses built upon the alum shale bedrock, did not have high radon levels [5].

2.1.6 Activated charcoal and HPGe detector

An experiment of measuring the emanation coefficient of rocks, building material and soil samples in Austria was conducted by Bossew 2003 [8]. Materials chosen as building materials were bricks, ceramics, gypsum boards and slag that is used for floors. The soil, stone and sand samples were taken from various areas in Austria in order to represent the different geological regions. The accumulation chamber method was used [11] and the samples were crushed to reduce their grain sizes to less than a few millimetres and to also increase the surface area. Activated charcoal detectors were used for absorbing the radon building up inside the chamber. These detectors can only take measurements for a short period of time of about a few days. The chamber was tightly sealed for about three weeks for the ^{226}Ra and the short-lived daughters to reach secular equilibrium. Gamma ray spectrometry method using an HPGe detector (Canberra, 19% relative efficiency) was used for obtaining the activity concentration of ^{226}Ra from the full-energy peaks of ^{214}Pb and ^{214}Bi at energies of 295, 352, 609 and 1120 keV. The values of emanation coefficient obtained were 0.20, 0.060 , 0.025, 0.0060, 0.0080 and 0.30 for dry soil and stones, sand, bricks, ceramic tiles, mineral slag and gypsum respectively. The experiment was conducted at room temperature at about 20 $^{\circ}C$ to eliminate the dependency of radon exhalation on temperature [8].

2.1.7 E-PERMs and HPGe detector

A study by Speelman 2004 [63] was performed in South Africa to determine the radon emanation of soil at the Kloof mine dump. In the study various techniques were used to determine the emanation coefficient, which included Electret Passive Environmental Radon Monitors (E-PERMs) and the HPGe detector. The types of Electret Ion Chambers (EIC) used in the study were the SST and the LLT chambers, where the SST refers to an S chamber fitted with a short term electret and the LLT refers to an L chamber fitted with a long term electret. The chamber type that was used determined the duration of the measurements in the jar. The S chamber allowed for 7 days measurement whereas the L chamber allowed for 1 month measurements. The samples having mass of 30 - 40 g were dried and left for one week and then put in a small petri dish and placed in the accumulation jar together with the E-PERMs. After the period of exposure the electrets were collected and the final voltages were read using the electret voltage reader, so that the radon concentration in the jar could be calculated. The accumulation method was used for the RnERaC (Radon Emanating ^{226}Ra Concentration) measurements which is given in $Bq.kg^{-1}$.

In the same study, radon concentration was measured at different depths at the Kloof gold mine dump using a RAD7 radon monitor. The results obtained were compared with the results of the one dimensional steady state model. Soil samples were taken at 5 cm, 50 cm and 100 cm in the same holes that the depth measurements were performed. The samples were oven dried at 105 $^{\circ}C$ and transferred to Marinelli beakers which were then sealed and stored for three weeks to obtain secular equilibrium. For determining the radium content of the soil samples the HPGe detector was used. The ratio of the RnERaC and the ^{226}Ra activity was used to calculate the radon emanation coefficient. The values obtained for the emanation coefficient at those depths were 0.16, 0.22 and 0.36, respectively. It was noticed that the emanation coefficient increased with depth [63].

2.1.8 HPGe detector

A study was conducted by Hassan et al.,2009 [23] to measure the emanation coefficient in samples of rocks, soils and building materials. The sample materials were oven dried at 105 $^{\circ}C$ to remove moisture, then placed in a container and subsequently sealed to avoid radon leakages. They were stored for a month to achieve secular equilibrium between radon progenies and ^{226}Ra. A hyper pure germanium (HPGe) detector was used for measuring the radium activity of the samples using the full-energy peaks of ^{214}Pb at 352 keV and ^{214}Bi at 609 keV. A closed chamber method was used for measuring the maximum radon concentration that had built up over time [11]. The radon emanation coefficient was then determined as the fraction of the radon activity concentration (Bq) and radium activity concentration (Bq). The emanation coefficient values obtained were in the ranges of 0.021 - 0.32, 0.0014 - 0.80, 0.0010 - 0.58 for rocks, soils and building materials, respectively. It was found in the experiment that the emanation coefficient increased with an increase in water content until the point of saturation in the pore space and decreased for dry conditions. An increase in temperature and decrease in grain size also increased the emanation coefficient [23].

2.1.9 RAD7 and HPGe detector

A similar study to Speelman 2004 was conducted by Ongori 2013 [47] in South Africa at the Kloof mine dump to measure the radon emanation coefficient and radon exhalation. The soil samples were extracted at different depths and the radon soil gas concentration was measured at the mine dump using the RAD7 radon monitor. About thirty-four soil samples were transported to the laboratory for analysis. The ^{226}Ra activity was then determined after some time had passed and secular equilibrium was achieved. The soil sample with a mass of 487.9 grams was put in an accumulation jar together with the S chamber (short term electret). The jar was used for the RnERaC (Radon Emanating ^{226}Ra Concentration) measurement, which is the concentration of the fraction of ^{226}Ra in the soil releasing the radon. The radium content of the soil sample was measured using an HPGe detector. The ratio given by the RnERaC and the ^{226}Ra activity gave the emanation coefficient of 0.28 [47].

2.1.10 Pylon AB-5 and HPGe detector

Shiroma et al.,2015 [60] measured the radon emanation coefficient of three types of soils in Okinawa, Japan. Soil samples were taken from nine different places, dried and sieved using a 2 mm mesh. The soil samples were then sealed in an accumulation chamber for 24 hours. The Pylon AB-5 radon monitor was used to measure the radon concentration in the chamber. At equilibrium condition the radon concentration was calculated using the following equation:

$$A_{eq} = \frac{A(t)}{1 - e^{-\lambda.t}} \tag{2.2}$$

where t represents the accumulation time (s), A(t) is the radon concentration $(Bq.m^{-3})$ at time (t) and λ is the radon decay constant (s^{-1}). For the determination of the radium activity concentration, the sealed soil samples were stored for 40 days in order to achieve equilibrium between ^{226}Ra and ^{222}Rn. Gamma spectroscopy using a HPGe detector to detect the full-energy peaks of ^{214}Pb (352 keV) and ^{214}Bi (609 keV) was used to determine the radium concentration. The radon emanation coefficient (f) was then determined using the following equation:

$$f = \frac{A_{eq}V_a}{A_{Ra}M} \tag{2.3}$$

where V_a is the volume of the chamber (m^3), A_{Ra} represents the radium content of the soil sample ($Bq.kg^{-1}$), M is the mass of the soil sample (kg) and A_{eq} is the equilibrium radon concentration ($Bq.m^{-3}$) [60].

2.1.11 Summary of the Literature Review

Different techniques were employed to determine the emanation coefficient of radon in materials and the emanation coefficient of radon is unique for each material. What was common in the above techniques was using the accumulation method so that the radon can be built up inside a vessel. The samples were sealed for some time in order for the equilibrium between radium and radon to be obtained. Different authors suggested that the samples should be stored for some time before measurements, some suggested two weeks and others one month (Moore and Moore 1984, Greeman and Rose, 1996). From these two suggestions the determination of radium activity concentration is time consuming and during the storage period some radon may leak out or get adsorbed into the samples. These artefacts could be minimized by making the sampling time to be less than 20 hours and that crushed samples should be used when determining the radon emanation coefficient of materials [19]. For this study the suggested sampling time would not be possible as the samples will be collected and taken to the laboratory for analysis. The half-life of radium (1600 years) which is the immediate parent of radon is much longer than that of radon (3.8 days), hence in order to measure the activity of radium, secular equilibrium has to be achieved between radon and radium and that can be obtained after about six half-lives (24 days) of the daughter nuclide.

The gamma-ray spectroscopy method was used for measuring the radium concentration in different materials. The effect of factors like the soil porosity, grain size, soil temperature and moisture content were also investigated in the experiments as they influence the radon emanation coefficient. An increase in the moisture content and soil porosity lead to an increase in the emanation coefficient and smaller grain sizes also resulted in high emanation coefficient of the sample materials. These factors are important in the measurement of the radon emanation coefficient and hence they need to be considered. The samples were crushed to increase the surface to volume ratio and to increase the diffusion length as well as porosity (which is the empty spaces in the soil) in order to get high values for the emanation coefficient. In this study the samples were not crushed.

Sakoda et al.,2011 [54] compiled a review on different studies that were previously conducted to evaluate the radon emanation coefficient of minerals, rocks, soils, mill tailings (uranium mill tailing) and fly ashes. The average values of the emanation coefficient were 0.03, 0.13, 0.20, 0.17 and 0.030 for minerals, rocks, soils, mill tailings and fly ashes, respectively [54]. UNSCEAR (2000) stated a value for the emanation coefficient of 0.20 for soil in the range of 0.01 - 0.8. Nazaroff and Nero (1992) reported the emanation coefficient value of 0.050 - 0.25 for soils [44]. De Martino et al.,(1988) [17] measured a value of 0.060 - 0.60 for soil samples. Ingersoll (1983) measured the value of the emanation coefficient of 0.28, 0.010 - 0.060 and 0.25 for gypsum, brick and soils, respectively [28]. Rogers and Nielson (1988) proposed that the average value of the emanation coefficient for most soils may be about 0.22 [52].

2.1.12 Motivation of the study

This study is motivated by the fact that radioactivity has always been part of our environment and we cannot eliminate it from the environment. What we can do, is to find ways of reducing its harmful effects on human beings. The present study is part of the proposed study on radon

in houses in South Africa. The knowledge of the emanation coefficient can help in making the sampling more efficient to eventually reduce the radon risk. In South Africa, where there are areas of concerns, in the Western Cape (Paarl area) are granite outcrops and mining activities that have been going on for over 100 years in the country could lead to elevated levels of natural radionuclides. As can be seen from Table 1.1, granite and shale rocks have higher contents of radionuclides implying the soil derived from those rocks will also have the higher levels of these radionuclides. In view of this, the spatial variability in the radon concentration could help in identifying areas that pose a radon risk. It has been found that the main source of radon indoors is the soil and rocks beneath the houses [44].

2.1.13 Aims or objectives of the study

The aim is to determine the radon emanation coefficient for soil samples collected in different locations in South Africa. In order to achieve this, different techniques were used including alpha and gamma spectroscopy to determine the radon and radium activity concentrations, respectively.

2.1.14 Problem Statement

The ground is the main source of the radon that gets inside houses thus the rocks and soils with high uranium content can produce high level of radon gas. High radon levels in the ground pose as a human health hazard due to the mobility of radon gas and when it is exhaled to the ground surface it can migrate into houses. High radon levels are hazardous to underground mine workers and house occupants in situations where there are poor ventilation systems and long exposure periods. High radon levels in the soil gas can be correlated to high radon levels in houses. This study is focused mainly on areas that have a high radon potential and hence only a few soil samples were collected in different places namely, Paarl (Western Cape) an area with granite outcrops, also in Boksburg (Gauteng) an old gold mine dump, Saldanha (Western Cape), West Coast (Western Cape), Richards Bay Minerals (KwaZulu Natal) and Kloof mine dump (Gauteng).

Chapter 3

Experimental details

3.1 Alpha and Gamma spectrometry

This chapter focuses on the measurement protocol and the different types of instruments used to conduct the experiments. The RAD7 is the main instrument for measuring the radon concentration, the HPGe and NaI(Tl) detectors were both used for intercomparisons of the radium activity concentrations. The measurement techniques are explained in detail below.

The first technique that was used in this study is alpha spectrometry using the RAD7 to determine the radon concentration. Alpha spectrometry is a method of measuring the energy of alpha particles emitted by the decays in the form of a pulse height distribution depending on their energy. The interaction between alpha particles and the detector is subject to statistical variations which results in the formation of a broadened peak.

The second technique that was used in this study is gamma spectrometry using the NaI(Tl) to determine the radium activity concentration. Gamma spectrometry is a method of measuring the gamma energies of many radionuclides at the same time in a bulk sample, and it is non-destructive. This method is not complicated and does not require time consuming radiochemical separations unlike for alpha spectrometry [51], [58], [26],[49]. The limitations of this method include the weak emission probabilities of many potentially useful emission lines, the relatively poor efficiency of the High Purity Germanium (HPGe) detectors over a wide range of energy and the difficult task of precisely calibrating the efficiency of the detector [31].
Gamma spectrometry is dependent on the creation of an electronic pulse which is proportional in magnitude to the gamma-ray energies of the emissions produced from the radioactive decay of a material being measured. Each radioactive material that emits gamma radiation has unique properties that can be used to both qualitatively identify the radionuclide present, and quantitatively establish the activity concentration of the material. There are cases in which the radionuclides do not decay by gamma emission, and hence these radionuclides cannot be measured directly by gamma spectrometry.

In measurements involving low activity samples but where the radionuclei present are known, the resolution of the detector may not be a limitation, for example in this work a NaI(Tl) detector is used in spite of its low resolution. In the case were high resolution is needed, a semiconducter gamma-ray detector that is able to deconvolute close full-energy peaks is used. An example of a detector with high resolution is the High Purity Germanium (HPGe) detector. The latest germanium detectors have typical Full Width at Half Maximum (FWHM) resolution of about 2 keV at the 1332 keV photopeak of ^{60}Co, and at lower energies a few hundred eV. The energy range that is useful for germanium detectors is from 5 keV to several MeV. The

HPGe may have a relative detection efficiency compared to the industry standard $3" \times 3"$ NaI (Tl) detector, of greater than 100% [10].

Radium activity in solid samples can be determined by gamma spectrometry via two modes, the direct measurement of the principal full-energy peak 186.25 keV for ^{226}Ra, and the indirect measurement from the gamma radiation of the decay products. The direct method has an advantage in that ^{226}Ra can be measured immediately after preparation without waiting for the decay products to build up. The difficulty of measuring ^{226}Ra directly is that it has a low intensity gamma-ray of only about 3.28% at 186.25 keV and also the presence of the ^{235}U photo-peak at 185.70 keV that has a stronger intensity of about 57.24%. These two peaks cannot be separated efficiently with the currently available HPGe spectrometers. In the case were no chemical separation is performed, ^{226}Ra can be quantified by using the 186.25 keV gamma peak by quantifying the contribution of the ^{235}U isotope to the doublet peak. This may be achieved using the ^{234}Th emissions or one of the low intensity emissions of ^{235}U, e.g. at 143.80 keV with a probability of 11.0%. Sample matrix effects, including self attenuation need to be considered when conducting these calculations. Alternatively, sophisticated deconvolution algorithms may be utilized to determine the respective contributions from each radionuclide.

On the other hand, the indirect measurement method is used to measure the decay products of different radionuclides e.g. ^{224}Ra, ^{226}Ra and ^{228}Ra isotopes. To determine the activity concentration of ^{226}Ra in environmental solids, radon (^{222}Rn) progenies i.e. ^{214}Pb and ^{214}Bi are detected using gamma spectrometry after an ingrowth period of at least 21 days. At this time secular equilibrium can be assumed after about five to seven times the half-life of ^{222}Rn ($t_{1/2}$ = 3.82 days) [12]. During this period the sample is hermetically sealed and stored to achieve secular equilibrium between ^{226}Ra and its progenies. Secular equilibrium is achieved when the activities of all the nuclides in the ^{238}U decay chain are equal. However, in natural materials the ^{238}U and the ^{226}Ra activities are not always equal as a result of geo-chemical processes. Due to the long half-life of ^{238}U of 4.5 billion years the ^{226}Ra is continously generated [34].
The decay rate of a radionuclide is given by its decay constant $\lambda = \frac{ln(2)}{t_{1/2}}$, where $t_{1/2}$ is the half-life of the radionuclide. In order to achieve secular equilibrium, the following has to be true:

$$t_{1/2}(parent) >> t_{1/2}(daughter) \tag{3.1}$$

For example, the half-life of (^{222}Rn) (3.82 days) is very small compared to that of ^{226}Ra (1600 years). Hence at secular equilibrium we have equal activities = λN

$$\lambda_{Ra} N_{Ra} = \lambda_{Rn} N_{Rn} \tag{3.2}$$

where, λ_{Ra} is the decay constant of radium, N_{Ra} is the number of radium atoms, λ_{Rn} is the decay constant of radon and N_{Rn} is the number of radon atoms.

3.1.1 Factors to consider when preparing and storing samples

The sample container used for gamma spectrometry must be tightly sealed, and the sample container should be impermeable to radon. Some of the commonly used sample containers for gamma measurements are polyethylene Marinelli beakers, jars, bottles and vials and non-plastics including aluminium. It is also important to ensure that the amount of free-air volume above the sample in the closed container is minimized. This reduces the amount of radon that may effuse from the sample into the air space, thus changing the counting geometry and the associated counting efficiency that applies to the gamma-emitting radon progeny.

When measuring environmental samples which are expected to have low activity, it is important to use large sample volumes to increase the sensitivity of the detector. The disadvantage of large sample volume is that it increases the path length of the photon. Another contributing factor to the path length of the photon is the chemical composition and density of the sample as this affects the self absorption in the sample. These factors eventually affect the efficiency of the detector. Hence, in order to obtain accurate quantitative data on the activity concentration of a radioactive material in the sample, it is necessary to correct for self-attenuation. Self-attenuation effects are more common in low energy photo-peaks associated with the uranium and thorium primordial series (especially ^{210}Pb and ^{234}Th when considering ^{226}Ra series measurements). However, there are different techniques that can be used to counteract the self-attenuation caused by the density and/or chemical composition of the material. Those techniques include semi-empirical methods, experimental determination of factors involving direct transmission and calibration methods [31], [2] and Monte Carlo based methods [68].

3.1.2 Radon concentration measurements

The closed chamber method shown in Figure 3.1 was used to determine the radon concentration [11]. Figure 3.1 shows the experimental setup which includes the RAD7 detector, the Durridge Drystik ADS-3, the vacuum chamber and the air tubes.

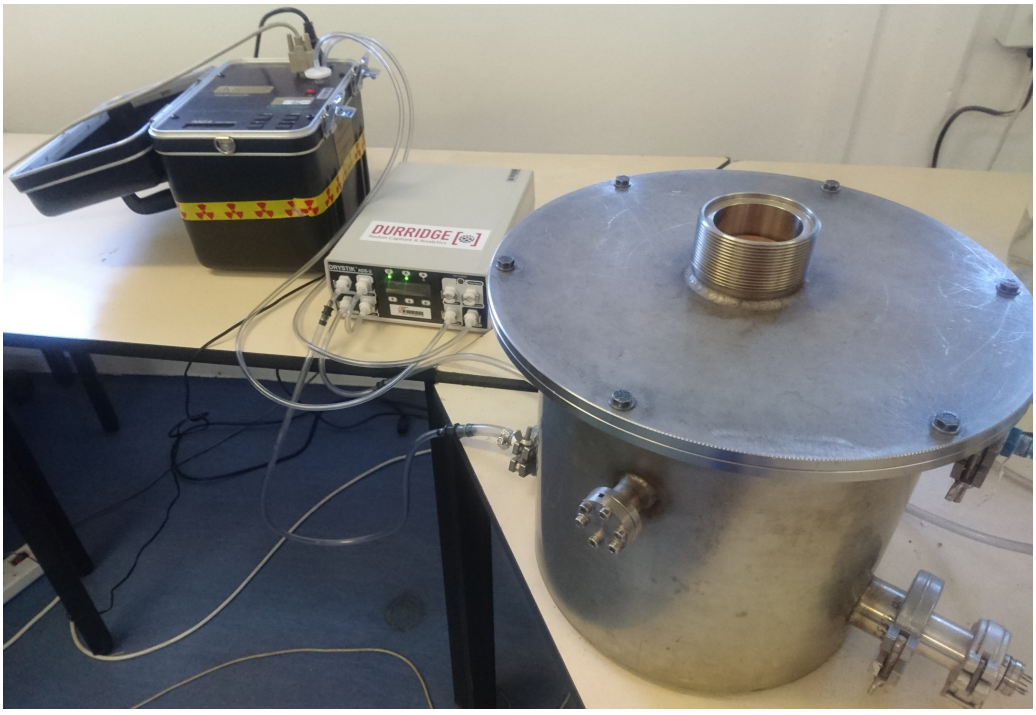

Figure 3.1: Experimental setup for radon concentration measurements.

In the chamber, a sample of sand was placed in an open dish. The sample thickness was small as compared to the diffusion length of radon in solid material of about 120 cm. Soil samples of different masses were measured for radon concentration, the first sample set with a mass of 0.256 kg, the second 0.512 kg and the third set with 0.768 kg. The same sample was measured twice to check the reproducibility of the radon concentration results. The chamber in Figure 3.1 has a volume of 12.5 L that volume was reduced by placing metal blocks to a volume of 6.2 L. This was done to reduce the number of days it took to get a measurable radon

concentration. Prior to measuring the radon concentration, the sample that was in a sealed plastic bag was opened and placed in an open dish overnight. The measurement was conducted the following day, by taking the sample with known mass and putting it in the accumulation chamber. After each sampling, fresh air was allowed into the chamber before taking another set of samples. This was done to make the initial radon concentration in the chamber to be negligible. It was also assumed that the radon decay in the pore space can be ignored since the sample thickness was very small compared to the diffusion length. The radon gas that has escaped from the soil gets into the chamber volume and is pumped through the pipes to the RAD7 radon monitor. The radon decay products are filtered out from entering the detector volume (see Figure 3.1). Then the RAD7 measures the average radon concentration built up over time.

3.1.3 Equations describing the radon build up inside the chamber

The change in the number of radon atoms (N) per time t (s) in the solid and gas phase in the closed chamber can be expressed as:

$$\frac{dN}{dt} = S - \lambda N \tag{3.3}$$

where S is the number of ^{222}Rn atoms that are created per second and gets into the air and λ (s^{-1}) is the decay constant of radon. Solving the above equation by separation of variables and integrating, the growth of radon is given by,

$$N(t) = \frac{S}{\lambda}\left\{1 - e^{-\lambda t}\right\} + N_0 e^{-\lambda t} \tag{3.4}$$

where N_0 is the initial number of radon atoms or background. It can be assumed that at $t = 0$ no radon atoms have decayed yet. Also considering the volume (m^3) of the chamber, the above equation can be written as:

$$\frac{N(t)}{V} = \frac{S}{\lambda V}\left\{1 - e^{-\lambda t}\right\} \tag{3.5}$$

The above equation can be interpreted as the radon concentration in the chamber,

$$C_N(t) = \frac{S}{\lambda V}\left\{1 - e^{-\lambda t}\right\} \tag{3.6}$$

where $C_N(t)$ is the radon concentration at time t in ($Atoms.m^{-3}$), and λ is the decay constant of radon (s^{-1}).
Thus the more useful activity concentration is given as follows:

$$C(t) = \frac{A}{V} = \frac{\lambda N}{V} = \frac{S}{V}\left\{1 - e^{-\lambda t}\right\} \tag{3.7}$$

The radon concentration in the chamber follows a linear growth during a certain build up period (see Figure 3.2). The build up in the chamber grows almost linearly for a period of two days, then follows an exponential trend due to the decay factor. If this trend is followed it also shows that there are no leakages in the accumulation chamber. Appendix A discusses the justification of this approximation.

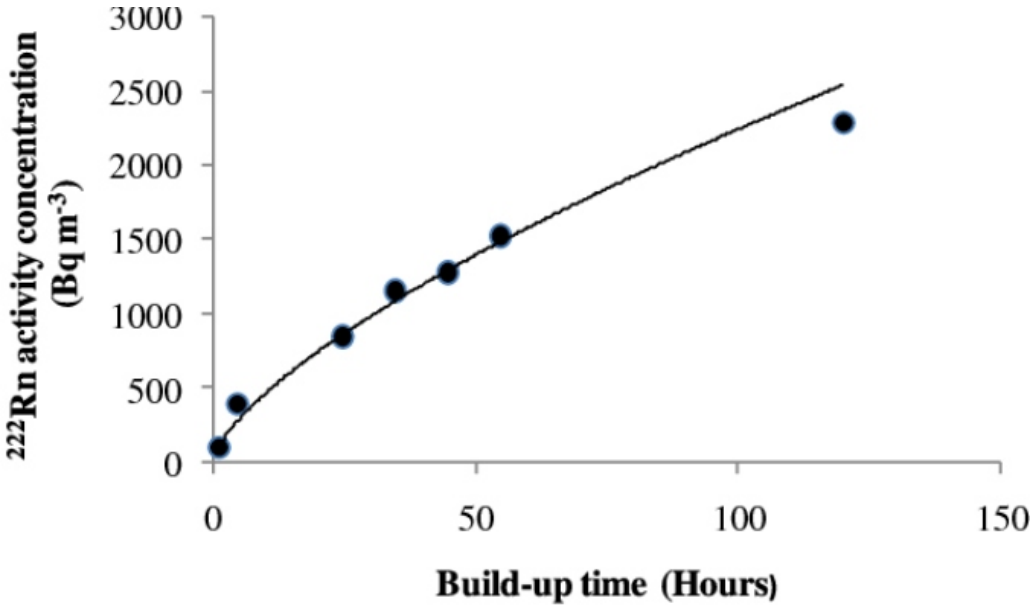

Figure 3.2: Variation of ^{222}Rn activity concentration with build-up time in the chamber [53].

In this study, measurements were conducted for about two days (i.e. during the mainly linear region of the accumulation curve) to determine the radon concentration (see Figures 4.5 & 4.6). From Equation 3.7 it is clear that the activity concentration will eventually saturate at $\frac{S}{V}$ but this will only be after about 7 half-lives of ^{222}Rn.

To get the average radon concentration in the chamber after a given time T Equation 3.6 is integrated:

$$C_{avg} = \frac{1}{T}\int_0^T N(t)dt = \frac{S}{V}\left\{1 - \frac{(1 - e^{-\lambda T})}{\lambda T}\right\} \tag{3.8}$$

Therefore, the average radon concentration ($Bq.m^{-3}$) in the chamber is given as,

$$C_{avg} = \frac{S}{V}\left\{1 - \frac{(1 - e^{-\lambda T})}{\lambda T}\right\} \tag{3.9}$$

The radon concentration can be modelled at time t for active methods, such as the RAD7 using Equation 3.7 by fitting the parameter S and (possibly) including the initial concentration as another parameter. Alternatively, the average measured value can be used to get S using Equation 3.9 [34].

3.1.4 Sampling and Preparation

Soil samples were collected from a depth of about 30 cm from the ground as suggested by Akerblom (1997) [19]. A spade was used to dig and extract the soil which was transferred to resealable plastic bags. The plastic bags were labelled appropriately with dates and locations for easy identification. Soil samples were collected from different locations which were selected by using a geology map of South Africa that shows uranium deposits and granite outcrops. The areas of interest for this study are, West Coast (Western Cape), Boksburg (Gauteng), Kloof (Gauteng), Paarl (Western Cape), Richards Bay Minerals (KwaZulu Natal), Saldanha (Western Cape) and Centurion (Gauteng). The total number of samples collected and analysed is fourteen. The samples were sealed and transported to the laboratory for analysis. Different techniques were used to analyze the alpha particles using the RAD7 and gamma-rays emitted by radon gas and its progenies using NaI(Tl). The alpha emitting nuclides that were studied are ^{218}Po at 6000 keV and ^{214}Po at 7670 keV and the gamma emitting nuclide used was ^{214}Bi with a gamma peak at 1764 keV. The ^{222}Rn concentration was detected using a continuous radon monitor the RAD7. The only drying that occurred was at room temperature while the samples were stored before taking measurements. The measurements were taken at room temperatures in order to keep conditions in the laboratory similar to those in the environment. Table 3.1 gives the locations coordinates of the places were samples were collected.

Table 3.1: Sample locations used in this study and their coordinates.

Locations	Sample Code	Coordinates		Date collected
		Latitude	Longitude	
Paarl (WC)	PP5	-33.73119	18.94778	17/10/2018
	PP6	-33.75409	18.95629	17/10/2018
Saldanha (WC)	SP1	-32.76265	18.02700	10/04/2019
	SP2	-33.00167	17.94028	10/04/2019
	SP3	-33.91833	17.98361	10/04/2019
	SP4	-33.00167	17.94028	10/04/2019
Boksburg (GP)	BP1	-26.21246	28.26175	29/10/2018
	BP2	-26.22572	28.23593	29/10/2018
	BP3	-26.23562	28.23617	29/10/2018
Richards Bay Minerals (KZN)	RBM	-28.75183	32.02214	26/08/2019
Centurion (GP)	CP1	-25.87939	28.18802	29/10/2018
Kloof Mine (GP)	KS51	-28.52978	29.80490	20/09/2010
	KS41B	-29.78583	30.82527	20/09/2010
West Coast (WC)	WC	-32.05868	18.88222	12/05/2015

The Figures 3.3-3.8 were taken from some of the locations were the samples were collected.

Figure 3.3: Paarl point 1 (PP5).

Figure 3.4: Paarl point 2 (PP6).

Figure 3.5: Saldanha point 1 (SP1).

Figure 3.6: Saldanha point 2 (SP2).

Figure 3.7: Boksburg point 1 (BP1).

Figure 3.8: Boksburg point 2 (BP2).

All the soil samples that were collected were put in the Marinelli beakers, sealed and stored for a period of 21 days (see Figure 3.9).

Figure 3.9: Sealed Marinelli beakers containing soil.

The empty Marinelli beaker was weighed first using a Dune compact balance (DCT5000) capacity 5000 g, then weighed again with the soil sample. The mass of the empty beaker was subtracted from the mass of the beaker with soil to give the mass of the soil sample in kg. A copper lid was placed on top of the soil inside the beaker, then sealed with lid. The sample was then made airtight by sealing it with a marine silicone sealant on the lid and stored for at least 21 days before measuring.

3.1.5 Techniques for analysing spectra

Two methods are used often in analysing spectra: peak or window analysis and full-spectrum analysis (FSA) [25]. In the former method, the net counts of the window around individual gamma peaks associated with the decay products of ^{238}U, ^{232}Th and the decay of ^{40}K are used to determine the activity concentration [32]. In the latter, almost the full energy spectrum is considered and the measured spectrum is described as the sum of the three common spectra of ^{238}U, ^{232}Th and ^{40}K, respectively. In this study, the windows also known as peak method was used to analyse the spectra. In the windows method only some regions of interest (ROIs) of the spectrum are considered, which are the area around the most prominent gamma peaks of the decaying nuclides. The net counts were obtained by integrating the peak area which is already calculated by the software. Those net counts were used to calculate the activity concentration ($Bq.kg^{-1}$) of the sample.

The following expression was used to calculate the radium activity concentration,

$$A = \frac{C_{net}}{Br.t_s.m.\epsilon} \tag{3.10}$$

where C_{net} is the net counts minus the background, Br is the branching ratio (probability of decay via gamma decay), t_s is the live time (s), ϵ is the full-energy peak detection efficiency and m is the mass of soil (kg). The full-energy peak efficiency of the given geometry is required for accurate calculations of the activity concentration. For the HPGe measurement, the Environmental Research Laboratory at iThemba LABS has found efficiency for the Marinelli beaker geometry by using standard sources from the International Atomic Energy Agency (IAEA). The results from the iThemba LABS laboratory for some strong sources were used to find the efficiency normalisation for the NaI(Tl) detector used in a lead castle at the University of the Western Cape (UWC). The radon emanation coefficient was determined using the following equation:

$$E = \frac{S}{A.m} \tag{3.11}$$

where S is the number of ^{222}Rn atoms that are created per second as described in Equation 3.3, A is the radium activity concentration and m is the mass.

3.1.6 RAD7 detector

The RAD7 is a robust, continuous real-time radon monitor, manufactured by Durridge Company Inc (www.durridge.com). It measures only the radon progeny formed by the decay of radon in the detector chamber. The continuous monitor allows for the variations in the radon concentration to be observed during a measuring period [24]. It allows for the detection of ^{222}Rn alpha emitting progenies i.e. ^{218}Po and ^{214}Po and ^{220}Rn progenies by the use of a silicon detector [56], [41]. In this study the RAD7 is used to measure the ^{222}Rn decay progenies only. The RAD7 contains an internal pump which pumps air at the flow rate of 0.6 $L.min^{-1}$ into the chamber [35]. Due to the electric field in the chamber the positively charged decay products of radon (^{218}Po and ^{214}Po) are collected on the detector surface. The alpha decays of these nuclei are counted as the measure of the radon concentration in air [64], [70].

Prior to measuring radon concentration using the RAD7, it is very crucial to purge the detector for at least 10 to 15 minutes [41]. This is done to reduce the relative humidity (RH) inside the detector and to remove any residual alpha emitters from previous measurements. The process of purging is done by a pump in the detector, which pumps fresh air into the chamber through a drying unit i.e. a Durridge DRYSTIK ADS-3 in this case. The Durridge DRYSTIK is an active moisture exchanger accessory for the RAD7. It has a Nafion membrane which is made of Teflon laced with hydrophilic molecules that passes water molecules from one to another down a humidity gradient in the material. The air in the membrane tube of the DRYSTIK ADS-3 is compressed which makes it possible for water molecules to cross the purge sheath even if the sheath is filled with fresh air at ambient humidity. Thus the system will start to dry incoming ambient air even without dry purging air in the sheath. If the dryer outlet air is circulated back to become purged air it will increase the efficiency of the drying process and the system becomes regenerative, bringing the air leaving the membrane tube to steadily lower humidity. The DRYSTIK ADS-3 can be used without a desiccant and it can reduce the relative humidity to less than 10%.

Inside the RAD7 there is a chamber that contains the detector. An electric field is created in the chamber at a high voltage. During the decay of radon, its progenies that are positive

ions ($^{218}Po^{+}$ and $^{214}Po^{+}$) are pulled by the electric field and may be deposited on the detector, which is at ground potential. The humidity in the chamber must always be low during the measuring period; below 10% to attract nearly all the positive ions. The detection efficiency of the RAD7 decreases as humidity increases due to the neutralization of polonium ions by water particles.

The RAD7 has an air filter outside to stop the solid radon progenies from entering the chamber and contaminating the detector. The air in the chamber will pass through to the outlet, which is connected by tubes to the accumulation chamber to form a closed loop. The alpha particles from the decay of the polonium ions hit the sensitive surface of the detector, thus producing the signals proportional to the alpha energy. The RAD7 is able to differentiate different radionuclides by their alpha energy using alpha spectroscopy, (see Figure 3.11).

The operating panel of the RAD7 detector must not be exposed to excess moisture. The connection tubes should be connected tightly to avoid air leakages during the measurement and to avoid suction of liquids into the inlet tube of the RAD7 detector. The RAD7 operates at its optimum level when the humidity is less than 10% [56], [41] and can measure radon concentration below 4 $Bq.m^{-3}$. In this study, the humidity was kept at less than 10%. The RAD7 radon monitor and its schematic is shown in Figure 3.10

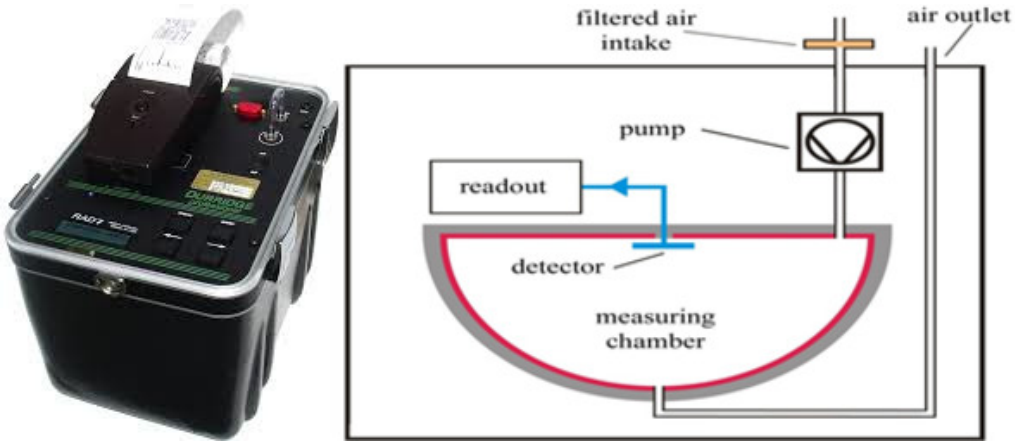

Figure 3.10: A picture of RAD7 radon monitor on the left and its schematic diagram on the right [41].

The RAD7 is categorized under solid state alpha detectors. A solid state detector is a semiconductor material (usually silicon) that changes the alpha radiation directly to an electrical signal. The usefulness of a solid state detector is its ruggedness. This type of detector has a good resolution and can also determine electronically the energy of each alpha particle. This helps to identify which isotope (^{218}Po, ^{214}Po, *etc.*) produced the radiation. The discrimination allows to differentiate between new and old radon and signal from noise. It can also distinguish between the alpha particles from ^{222}Rn decay products and ^{220}Rn decay products. This technique known as alpha spectrometry, can be used in sniffing, or grab sampling applications. The RAD7 has a very small background and it does not have the problem of the building up of ^{210}Pb in the detector chamber like in other detectors [41].

The RAD7 has an internal sample chamber of 0.7 L hemisphere, coated on the inside with an electrical conductor, having the silicon alpha detector at the centre of the hemisphere. The inside of the conductor is charged by the high voltage power circuit to a potential of 2000 to 2500 volts, relative to the detector, creating an electric field throughout the volume of the cell [41]. The RAD7 amplifies, filters, and sorts the signals according to their strength. In sniff

mode, the RAD7 uses only the ^{218}Po signal to determine ^{222}Rn concentration after three hours and the ^{216}Po signal to determine thoron concentration. The RAD7 can also be used in screen testing for rapid response to the radon concentration. In the normal mode, the RAD7 uses both the radon alpha emitting progenies ^{218}Po and ^{214}Po to determine the ^{222}Rn concentrations for better precision. The auto mode is used for long term measurements and the indication changes from sniff to normal after three hours of the measurement. The RAD7 manual recommends that the AUTO mode be used for all screening tests and any tests to measure the average concentration over a period of time. In this study thoron was not considered, since the aim of the study is to measure ^{222}Rn concentrations. The RAD7 achieves a fast response to changes in ^{222}Rn concentration, and a fast recovery from high concentrations [41].

This radon monitor can measure alpha energies in the range of 0 to 10 MeV. In this study the region of interest is from 6 to 9 MeV for the alpha particles emitted from ^{218}Po and ^{214}Po. Though the RAD7 detects the radiation from radon progenies internally, the only measurement it makes is of the radon gas concentration. An electrical signal is created by the alpha particles in the detector. This signal is then amplified and converted to digital form. The microprocessor in the RAD7 picks up the signal and stores it in its memory according to the energy of the particle to form a spectrum (see Figure 3.11) [41].

The RAD7 groups the spectrum into a series of 200 individual channels, each representing 0.05 MeV. After the RAD7 detects an alpha particle, it increments one of these 200 channels by one. The channels are grouped into 8 windows (labelled A-H) to simply analyse the spectrum (see Figure 3.11). Window A covers the energy range of 5.40 to 6.40 MeV, which includes the 6.00 MeV alpha particles from ^{218}Po decay. Window B covers the count rates from ^{216}Po decay (6.78 MeV), window C covers the count rates from ^{214}Po decay (7.69 MeV), and window D covers the count rates from ^{212}Po decay (8.78 MeV). Windows A and C are used to derive the radon concentration using the normal mode, whereas windows B and D account for the thoron concentration, which is not considered in this study.

To convert raw spectral data to a radon concentration value, all the counts in each window must be summed and divided by the detector measuring time and efficiency during data collection. This is all stored in the memory of the detector. A typical alpha energy spectrum is shown in Figure 3.11.

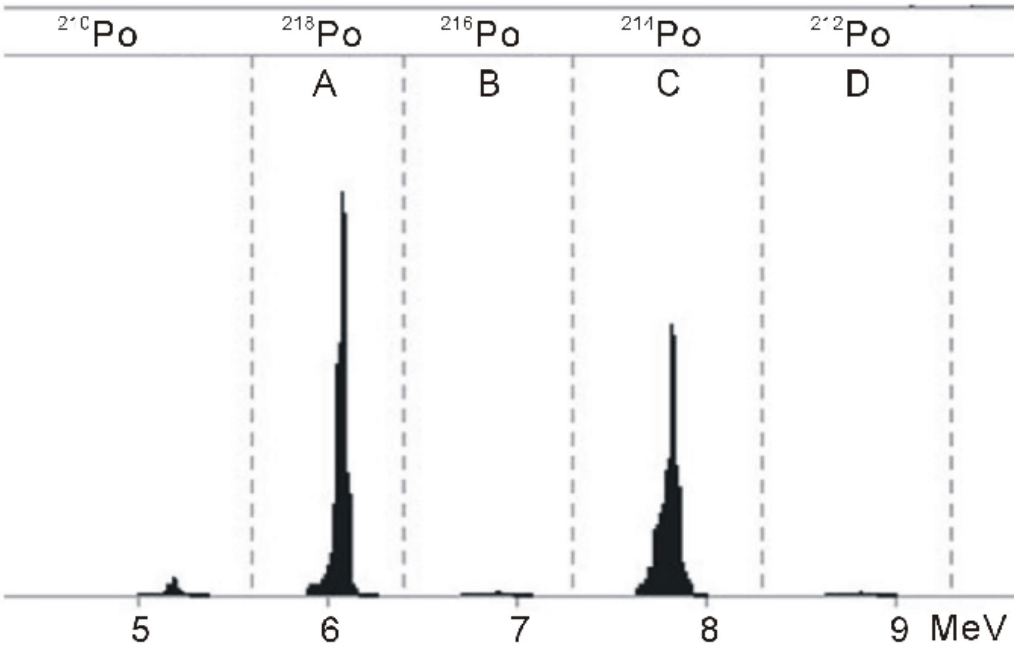

Figure 3.11: Alpha Energy Spectrum [3].

The RAD7 provides a printed cumulative spectrum after every radon measurement that includes windows A-D (see Figure 3.11). Windows E-H make up the composite window O. Window O is the sum of all the counts arising from energy ranges of windows E-H. The counts from window O are due to the noise in the system and these counts are ignored [41].

3.1.7 Radium content measurements

The radium activity concentration was obtained by measuring with a 7.5 cm × 7.5 cm NaI(Tl) detector at the University of the Western Cape. The samples in the Marinelli beaker were placed in a lead castle of 8 cm thickness as shown in Figure 3.12. These measurements were gradually checked by re-measuring a few samples using the hyper-pure germanium (HPGe) at the National Nuclear Regulator and at iThemba LABS. The HPGe detector has a better energy resolution than other gamma ray detectors e.g NaI(Tl). The HPGe detector at iThemba LABS is arranged in a way to measure low activity samples of either solids or liquids. The detector crystal is housed in a lead castle that is 10 cm thick in order to shield against background radiation. The lead castle is lined with sheets of copper to attenuate the low energy X-rays emitted by the lead, the same as the lead castle housing the NaI(Tl) detector at the University of the Western Cape.

The gamma measurements were started after the 21 days period of storage was over. These measurements were performed by using a NaI(Tl) detector to measure the radium activity of the soil samples. The samples were counted for twenty-four hours. The net counts from the full-energy peaks of ^{214}Bi at 1764 keV and ^{208}Tl at 2615 keV were used for determining the activity of radium and thorium in the soil. In this study only results from the full-energy peak of ^{214}Bi are reported. The winTMCA software was used for setting the regions of interest (ROIs). Then an Excel spreadsheet was used for further analysis and plotting of graphs. The type of detector that was used is the inorganic scintillation detector, namely a sodium iodide detector doped with thallium NaI(Tl) supplied by REXON. This detector has good detection efficiency since it has a $3" \times 3"$ ($75\ mm \times 75\ mm$) crystal even though it has relatively poor energy resolution. Its crystal is encapsulated in an aluminium casing connected to a photomultiplier

tube (PMT). The detector has a scintiSPEC multi-channel analyzer (MCA) attached at the back that also includes an amplifier and a source for high voltage and a single USB cable connecting the MCA to a PC. This type of detector is operated at room temperature. Figure 3.12 shows the experimental set-up using the NaI(Tl) detector at UWC containing the soil sample.

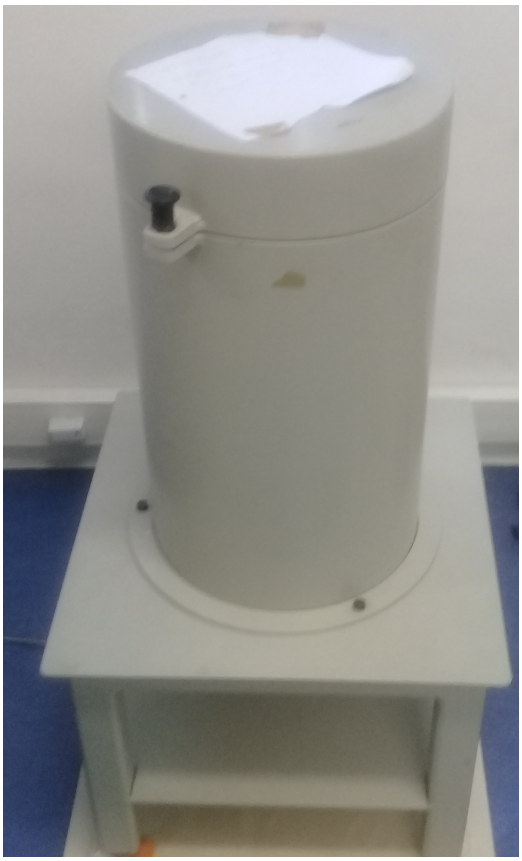

Figure 3.12: Lead castle that houses the NaI detector.

The NaI(Tl) detector is housed in a lead castle as shown in Figure 3.12 to attenuate the background radiation. Lead is effective in shielding against the background radiation due to its high atomic number and density. The castle has circular lead disks of 8 cm in thickness that forms a cylindrical shape. The top of the castle can be opened to place the beaker with the sample. At the bottom of the castle there is a hole which holds the detector and a cable that transfers the data to the computer. The background spectrum was characterised by two significant peaks in the thorium and uranium series that is ^{208}Tl (2614 keV) and ^{238}U (1764 keV), respectively. The NaI detector set-up is composed of the photomultiplier tube (PMT), multi-channel analyser and the photocathode. Each component's function is explained below. Figure 3.13 shows a schematic of the PMT.

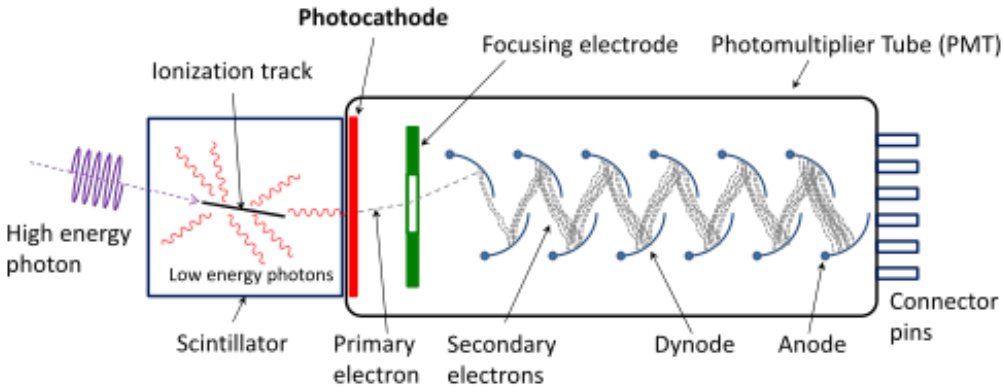

Figure 3.13: Schematic of the photomultiplier tube coupled to a scintillator [33].

3.1.8 Detector and photomultiplier tube

The NaI(Tl) scintillator is a sensitive detector of photons. The electrons created by the interaction of the gamma-rays in the crystal causes ionisation. At the photocathode incident photons from the source of typically 3 eV emit electrons from the surface by the photoelectric effect described in Chapter 1. The photocathode is a window that connects the PMT to the detector. Those electrons are then directed by the focusing electrode toward the electron multiplier, where electrons are multiplied by the process of secondary emission. The electron multiplier consists of a number of electrodes called dynodes. Each dynode is held at a more positive potential, by ≈ 100 Volts more than the preceding one. Materials which have negative electron affinity are usually used in the dynodes to increase secondary electrons. The geometry of the dynode chain is such that a cascade occurs with an exponentially increasing number of electrons being produced at each stage. This cascade of electrons is then collected in the anode to produce an electric pulse [36].

3.1.9 The multi-channel analyser (MCA)

The cascade of electrons that has been produced in the photomultiplier tube is collected at the anode and it produces a pulse. This pulse is sorted according to the pulse height of a particular channel in a multichannel memory. This is done by the MCA (TARGET USB MCA scintiSPEC in this case) by using the analog-to-digital converter (ADC) to convert the incoming pulse. The MCA then stores the digitized pulses in a memory channel whose address is proportional to the digitized value corresponding to pulse amplitudes. The gamma counts are then displayed as an energy spectrum and analysed using the winTMCA32 software. This software is equipped with a hardware setup option to set the gain and high voltage among other things. The gain was set to 1.5 and high voltage to 1050 Volts for the measurements in this work in order to display all the energy peaks from the natural decay series in 1024 channels [33].

3.1.10 Energy calibration

The winTMCA32 software records the counts versus channel number forming a spectrum. The spectrum that is acquired is then calibrated to get the correct energy of a particular channel. The system was calibrated with a source of known energy peaks. This was done directly by using the winTMCA32 software by selecting the energy calibration method and plotting the energy in a region of interest (ROI) versus the corresponding channel number where the peak occurs. To calibrate using two points, the software uses the equation of a straight line [36].

$$E = a(Ch) + b \tag{3.12}$$

where E is the energy at a particular channel Ch, a is the slope and b is the offset.
In the case of many available points to consider for energy calibration, the software uses a quadratic equation:

$$E = a(Ch)^2 + b(Ch) + c \tag{3.13}$$

where c is now the offset. In this study we used Equation 3.13.

3.1.11 Energy resolution

The ability of a detector to resolve peaks closely spaced in energy is important when taking measurements as it gives more information about the peaks. NaI(Tl) detectors have good energy resolution compared to other scintillators, but poor as compared to the semiconductors like HPGe. The energy resolution of a detector is given as a percentage of a full-energy peak's Full Width at Half Maximum (FWHM) over the centroid value of that particular energy peak. The smaller the percentage value the better the resolution. Any energy values separated by a value bigger than or equal to the detector's FWHM should be resolvable [33], [36]. The measurements in this work do not require very good resolution since we know the nuclei that are expected in the samples since they are natural materials. Thus the peaks are well-known and separation of close-lying peaks are not essential.

Figures 3.14-3.16 shows typical spectra obtained using NaI(Tl) detector, the marked peaks are the ones that were of interest for this study. The measurement period was 24 hours.

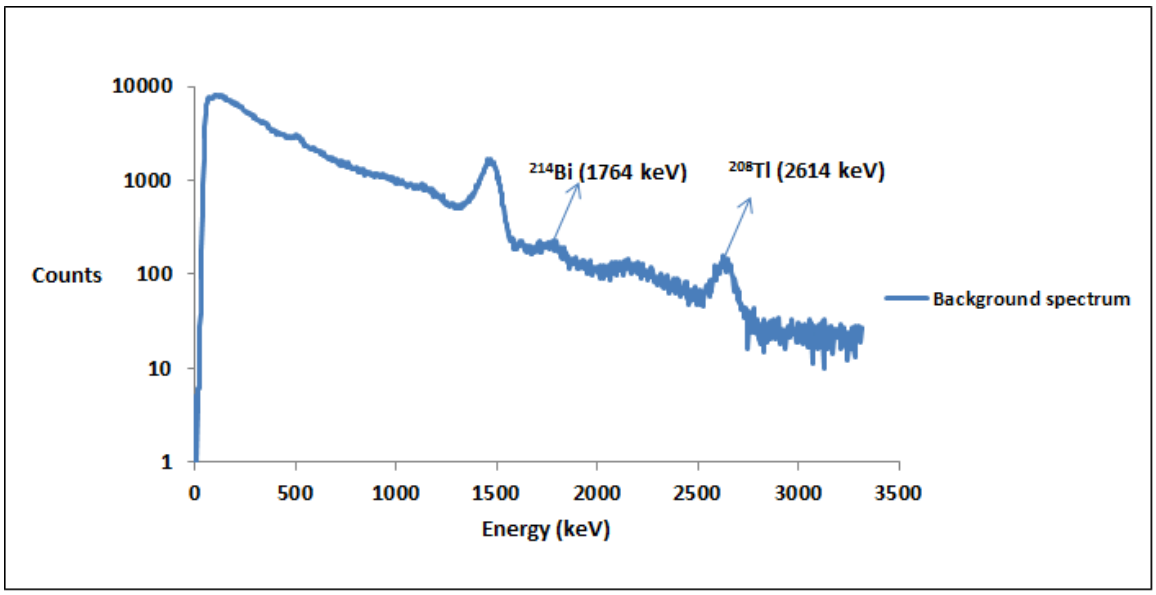

Figure 3.14: The spectrum of the background radiation (empty Marinelli beaker).

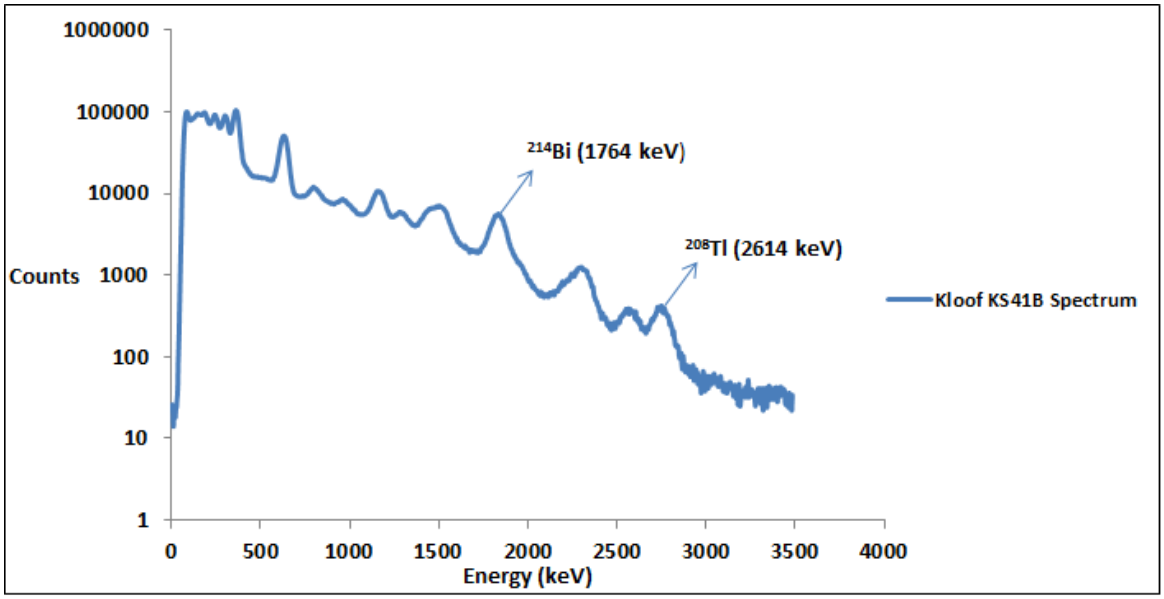

Figure 3.15: The spectrum of the Kloof mine dump sample (KS41B).

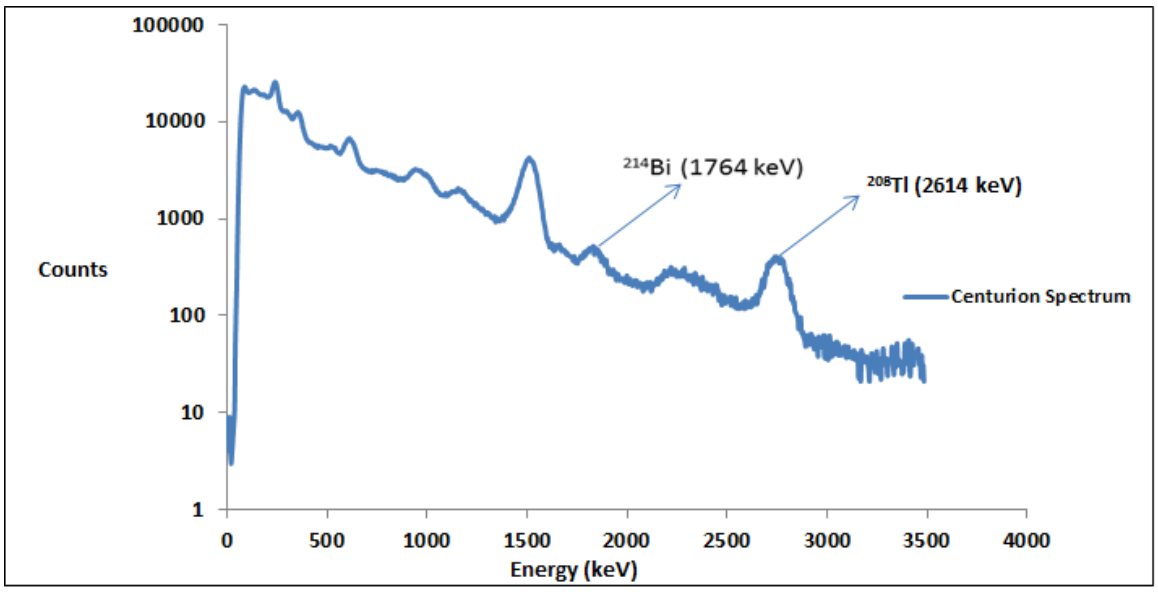

Figure 3.16: The spectrum of the Centurion soil sample (CP1).

3.1.12 Chi-squared minimisation

The expression that was used to fit the data as derived in Equation 3.7 is given below:

$$C(t) = C_0 e^{-\lambda t} + \frac{S}{V}\left\{1 - e^{-\lambda t}\right\} \tag{3.14}$$

The two unknown parameters, C_0 and S were obtained using a least squares method through Solver in Excel. These parameters are fixed at values that minimize the sum of the square of the difference between the measurement and the model. The goodness of the fits were analysed using the Chi-squared method, which considers the following equation [40]

$$\chi^2 = \frac{1}{N - M}\sum_{i=1}^{N}\frac{(\hat{y}_i - y_i)^2}{\sigma_i^2} \tag{3.15}$$

where $N - M$ is the number of degrees of freedom, $\hat{y}_i$ is the measured value and y_i is the model value, σ_i is the uncertainty in each value of the measurement and χ^2 is the Chi-squared value. For a good fit the reduced Chi-squared (χ^2) is expected to be close to one.

Chapter 4

Results and Discussion

4.1 Results

In this chapter the results obtained during the measurement of the radon concentration and the radium activity concentration are presented and the radon emanation coefficients are calculated.

4.1.1 The radon concentration measurement results

The average radon concentrations that were obtained from the RAD7 and the S values were calculated using Equation 3.9. Table 4.1, gives results of the radon concentration and S-values for soil samples of different masses. In Table 4.1, KS represents Kloof samples, BP represents Boksburg samples, PP represents Paarl samples, SP represents Saldanha samples, CP represents Centurion samples, WC represents West Coast samples and RBM represents the Richards Bay Minerals sample. The numbers represent the sampling point. The uncertainties in the S-values are similar to the uncertainties in the ^{222}Rn concentrations since the other parameters in Equation 3.9 are accurately known. The uncertainties in S-values are suppressed for ease of reading.

Table 4.1: Radon Concentration and S-values calculated. Note that the S-values increase with increasing mass as expected.

Sample	^{222}Rn Concentration $Bq.m^{-3}$			Extracted S values from Equation 3.9		
	0.256 kg	0.512 kg	0.768 kg	0.256 kg	0.512 kg	0.768 kg
KS51	225 ± 5	476 ± 7	745 ± 9	9	19	29
KS41B	352 ± 6	442 ± 7	639 ± 8	14	17	25
BP1	546 ± 8	2512 ± 17	3822 ± 21	12	55	82
BP2	175 ± 4	390 ± 7	492 ± 7	7	15	19
BP3	315 ± 6	1394 ± 12	2089 ± 15	22	99	156
PP5	204 ± 5	327 ± 6	703 ± 9	8	12	28
PP6	223 ± 5	316 ± 4	464 ± 7	9	19	29
SP1	99 ± 3	137 ± 4	196± 5	2	5	8
SP2	77 ± 3	144 ± 4	178± 4	3	6	7
SP3	61 ± 3	442 ± 7	237 ± 5	3	17	9
SP4	99 ± 3	181 ± 5	259 ± 5	4	7	10
CP1	58± 3	67 ± 3	218 ± 5	2	3	6
RBM	358 ± 6	176 ±4	221 ± 5	14	7	9
WC	233 ± 5	301 ± 6	467 ± 7	9	12	18

4.2 The radium activity measurement results

The measured values of the radium activity concentration, radon emanation coefficient and S-values are given in Table 4.2.

Table 4.2: Radium activity concentration and the emanation coefficient values of different soil samples.

Sample	^{226}Ra Activity $Bq.kg^{-1}$	Extracted S-values from Equation 3.9			Emanation Coefficient extracted from Equation 3.11		
		0.256 kg	0.512 kg	0.768 kg	0.256 kg	0.512 kg	0.768 kg
KS51	339 ± 51	9	19	29	0.102 ± 0.003	0.108 ± 0.003	0.113 ± 0.003
KS41B	368 ± 56	14	17	25	0.147 ± 0.003	0.092 ± 0.003	0.089 ± 0.003
BP1	1146 ± 173	12	55	151	0.073 ± 0.006	0.169 ± 0.011	0.171 ± 0.011
BP2	92 ± 14	7	15	19	0.313 ± 0.007	0.326 ± 0.007	0.275 ± 0.007
BP3	771 ± 116	22	99	156	0.063 ± 0.005	0.139 ± 0.005	0.139 ± 0.005
PP5	147 ± 22	8	12	28	0.214 ± 0.005	0.171 ± 0.005	0.245 ± 0.014
PP6	64 ± 10	9	19	29	0.541 ± 0.012	0.572 ± 0.010	0.373 ± 0.008
SP1	34 ± 5	2	5	8	0.276 ± 0.007	0.310 ± 0.007	0.296 ± 0.007
SP2	15 ± 2	3	6	7	0.780 ± 0.016	0.739 ± 0.011	0.609 ± 0.032
SP3	30 ± 5	3	3	9	0.395 ± 0.009	0.169 ± 0.003	0.405 ± 0.009
SP4	18 ± 3	4	7	10	0.847 ± 0.015	0.774 ± 0.015	0.738 ± 0.010
CP1	11 ± 2	2	3	6	0.812 ± 0.019	0.469 ± 0.010	0.686 ± 0.011
RBM	72 ± 11	14	7	9	0.765 ± 0.018	0.188 ± 0.006	0.157± 0.006
WC	$9.206 \times 10^3 \pm 1391$	9	12	18	0.004 ± 0.006	0.003 ± 0.0004	0.003 ± 0.0004

Table 4.3 gives the fit (Equation 3.14) values of Chi-squared, S-values extracted using equation 3.9 and C_0 which is the initial radon concentration in the chamber obtained using Solver in Excel. Most Chi-squared values are well below one, indicating that the RAD7 probably overestimates the uncertainties.

Table 4.3: Chi-squared values from the fit.

Sample	χ^2	C_0	S
BP1	0.6	51	19
BP2	0.3	51	5
BP3	0.4	3	12
PP5	1.5	78	5
PP6	0.3	15	7
CP1	0.3	21	2
SP1	0.3	48	2
SP2	0.4	16	2
SP3	0.2	23	2
SP4	0.3	59	2
KS41B	7	162	6
KS51	0.4	18	8
WC	1.1	1.1×10^{-6}	9
RBM	239	18	8

Figures 4.1 & 4.2 shows the radon concentration and radium activity concentration variations in different locations.

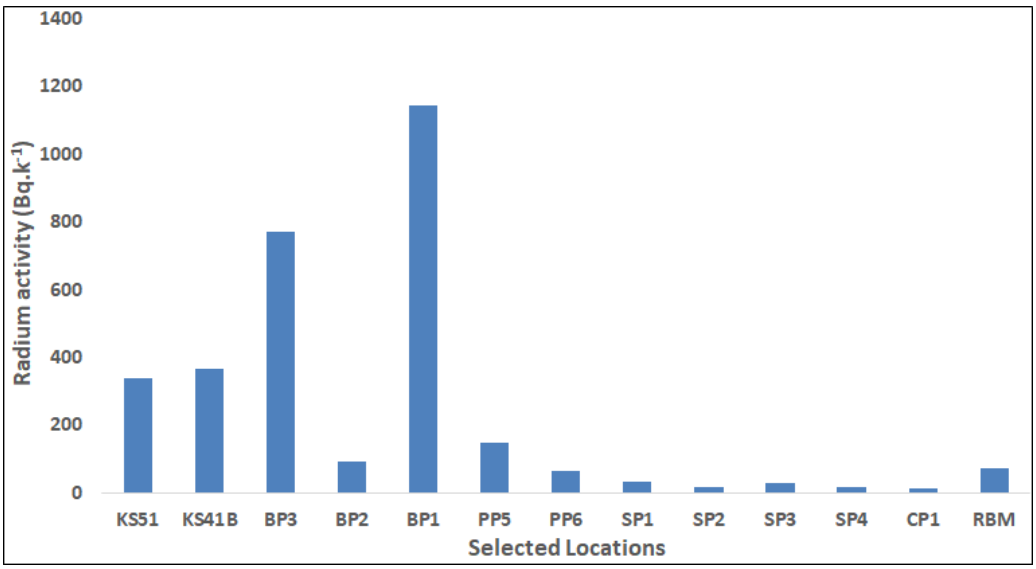

Figure 4.1: Radium activity concentration for soil samples at different locations.

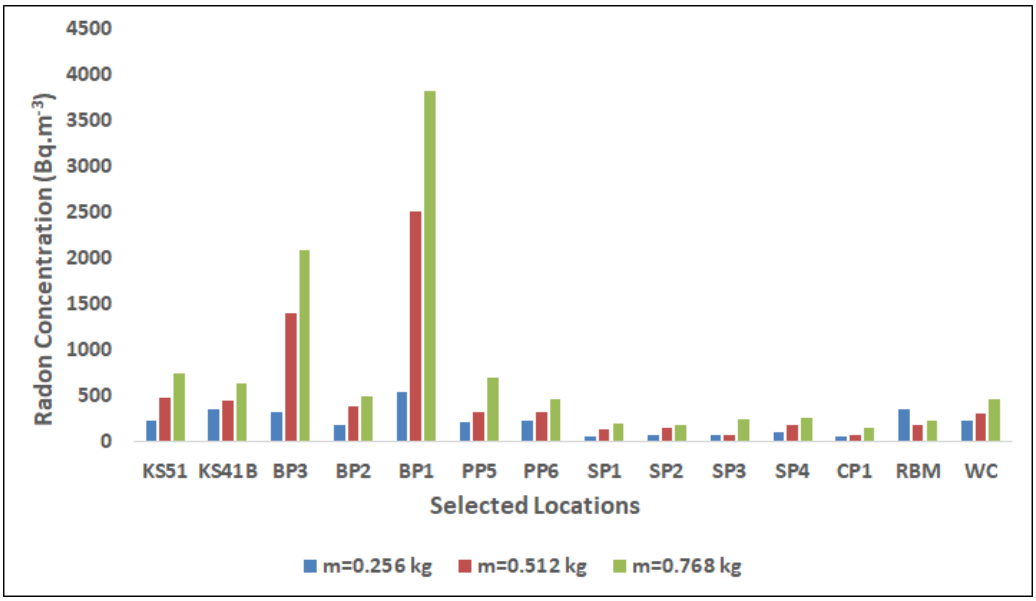

Figure 4.2: The radon concentration in soil air for different sample masses (0.256, 0.512, 0.768 kg) at different locations.

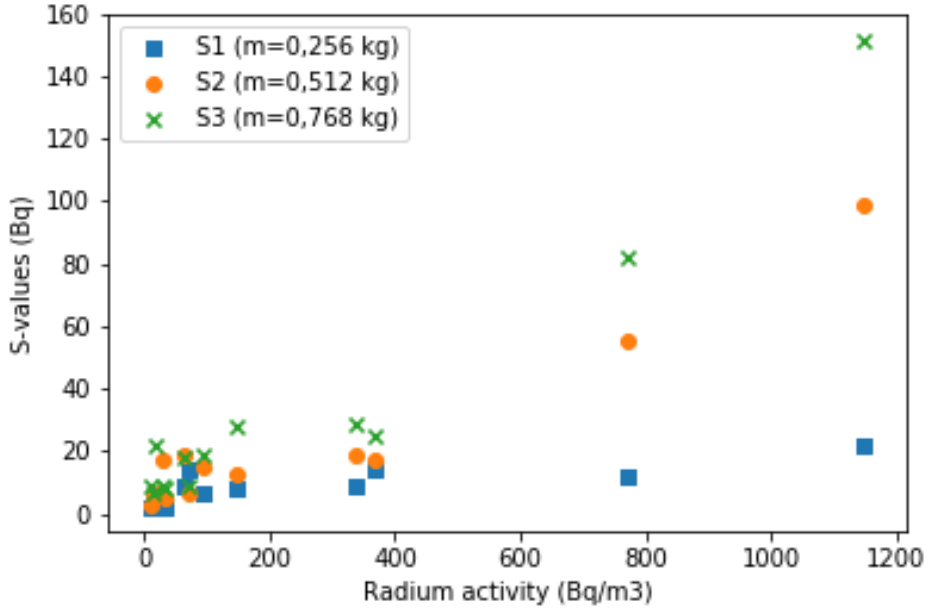

Figure 4.3: The relationship between the S-values and the radium activity in soil samples.

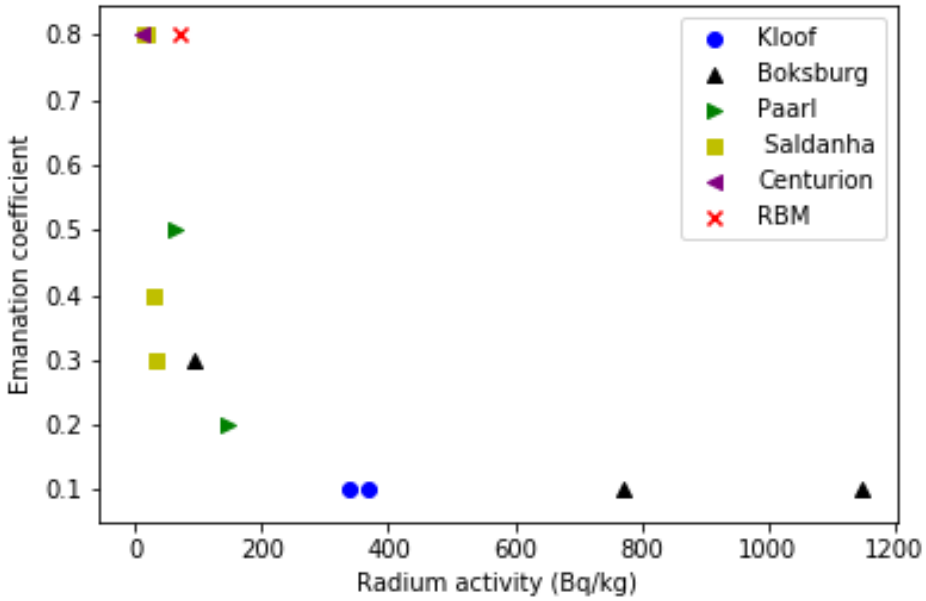

Figure 4.4: The relationship between emanation coefficient and the radium activity in soil samples.

Figure 4.3 shows the variation of the S-values and the radium activity concentration and Figure 4.4 shows the variation of the emanation coefficient and the radium activity.

Figure 4.5 shows the build up of radon concentration inside the chamber in a period of two days for Boksburg sample (BP3). Figure 4.6 shows the build up of radon concentration inside the chamber for a 185 kBq ^{226}Ra standard source.

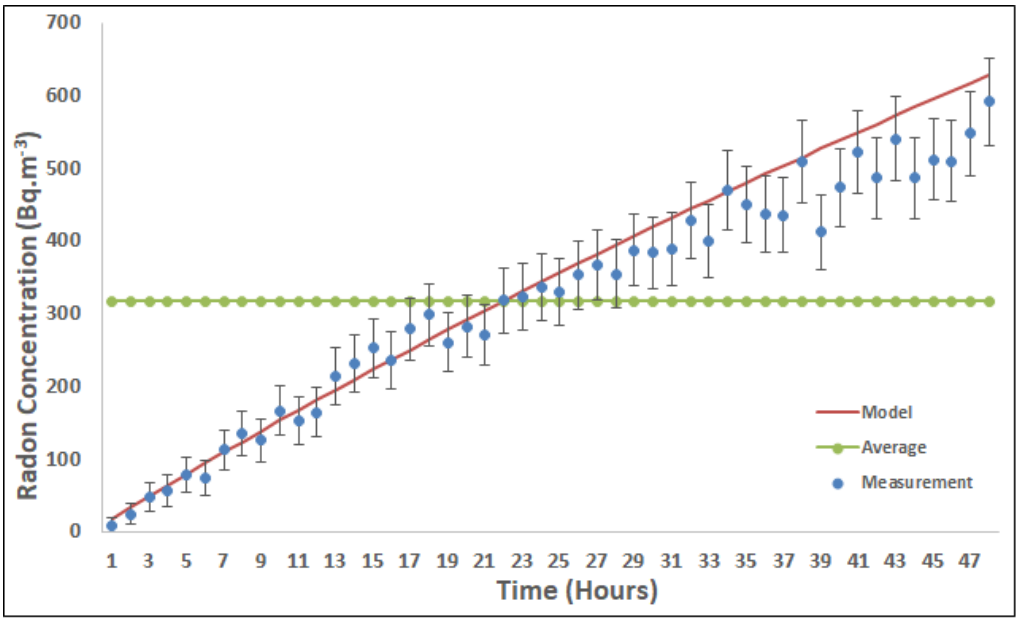

Figure 4.5: Radon concentration as a function of time for BP3 sample.

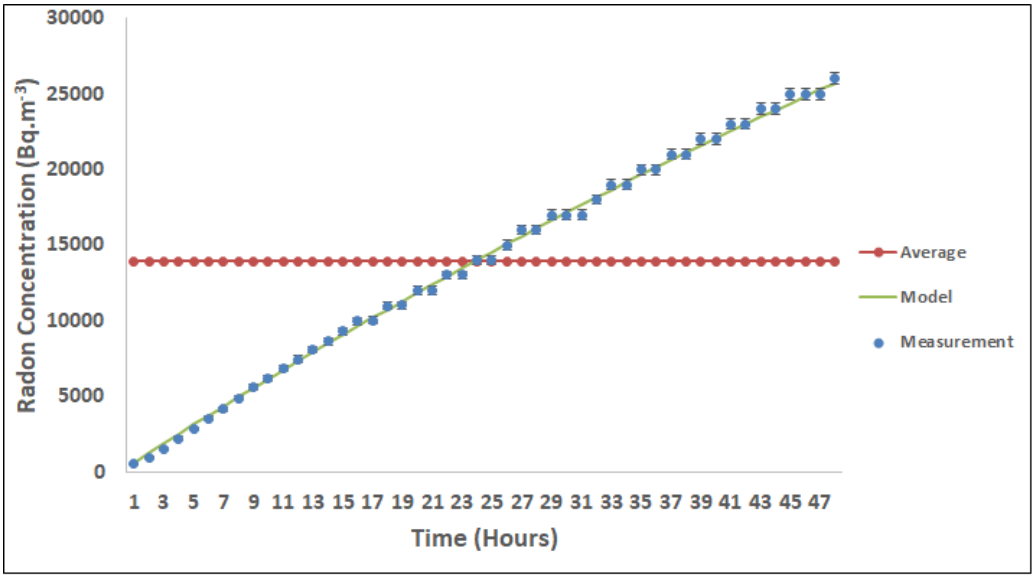

Figure 4.6: The radon concentration as a function of time using a standard ^{226}Ra source.

Figures 4.5 & 4.6 shows the measurement values (dots), the modelled values (line) and the average radon concentration (line with dot) for each soil sample, (see Appendix B) for more of the same graphs. Figure 4.6 shows the build up of radon concentration inside the chamber for a 185 kBq ^{226}Ra standard source. Figure 4.6 shows that there are no leakages in the chamber.

4.3 Discussion

In order to achieve the objective of this study, two different techniques were employed to determine the radon emanation coefficient. The commonly used method for measuring the radon concentration is by accumulation in a closed container. The samples were measured for a period of 48 hours in the chamber. Two parameters which are important for measuring the radon emanation coefficient of soil samples were considered. Those parameters are the radon concentration produced and the radium activity concentration. The first parameter was measured using a RAD7 radon monitor for quantifying the radon concentration inside the chamber. The average radon concentration in the chamber built up over 48 hours was recorded for each sample. Equation 3.9 was then used to calculate the S-values, which are the number of radon atoms that are created per second. The second parameter was measured using a NaI(Tl) detector to determine the radium activity concentration of the soil. The samples were sealed for 21 days to achieve secular equilibrium between radium and radon decay products. Afterwards they were counted using the NaI(Tl) detector for a period of 24 hours. The radon emanation coefficient was then determined from the S-values and the radium activity concentration using Equation 3.11. Table 4.4 gives the comparisons of the radium activity concentration measured using the NaI(Tl) at UWC, HPGe at iThemba LABS and also the HPGe at NNR.

Table 4.4: Comparison of the radium activity concentration results for a few soil samples, (-) indicates that no measurements made.

Sample	Results from this study A_{Ra} $(Bq.kg^{-1})$	iThemba LABS A_{Ra} $(Bq.kg^{-1})$	NNR A_{Ra} $(Bq.kg^{-1})$
KS52	328 ± 50	322 ± 15	204 ± 8
BP3	771 ± 116	-	465 ± 19
KS21	324 ± 49	323 ± 15	-
KS41	368 ± 56	350 ± 16	-

Intercomparison results using an HPGe detector at the NNR gave a lower value of the radium activity concentration than for HPGe at iThemba LABS and the NaI(Tl) at UWC. Intercomparison results using an HPGe detector from iThemba LABS gives similar results to those obtained from the NaI(Tl) detector.

From Table 4.1 it can be seen that the radon concentration increases with an increase in the mass of the samples as expected, except for the RBM sample due to unknown reasons. Also from Table 4.1, the extracted S-values from Equation 3.9, increases with an increase in mass, showing that more radon atoms are created in a bigger area of the soil. The radon concentration values obtained for the samples ranged from, 175 - 546 $Bq.m^{-3}$, 358 $Bq.m^{-3}$, 225 - 352 $Bq.m^{-3}$, 233 $Bq.m^{-3}$, 204 - 223 $Bq.m^{-3}$, 61 - 99 $Bq.m^{-3}$ and 58 $Bq.m^{-3}$ for Boksburg, Richards Bay Minerals, Kloof, West Coast, Paarl, Saldanha and Centurion, respectively for sample mass of 0.256 kg. The radon concentration values for sample mass of 0.512 kg ranged from, 390 - 2512 $Bq.m^{-3}$, 442 - 476 $Bq.m^{-3}$, 137 - 442 $Bq.m^{-3}$, 316 - 327 $Bq.m^{-3}$, 301 $Bq.m^{-3}$, 176 $Bq.m^{-3}$, and 67 $Bq.m^{-3}$ for Boksburg, Kloof, Saldanha, Paarl, West Coast, Richards Bay Minerals and Centurion, respectively. Finally, the radon concentration for sample mass of 0.768 kg ranged from, 492 - 3822 $Bq.m^{-3}$, 639 - 745 $Bq.m^{-3}$, 464 - 705 $Bq.m^{-3}$, 178 - 259 $Bq.m^{-3}$, 221 $Bq.m^{-3}$, 218 $Bq.m^{-3}$, and 18 $Bq.m^{-3}$ for Boksburg, Kloof, Paarl, Saldanha, Richards Bay Minerals, Centurion and West Coast, respectively.

In Table 4.2, radium activity concentration of the soil sample from West Coast is significantly high with the value of 9.206×10^3 $Bq.kg^{-1}$ due to the zircon in the soil which may have high uranium content. In Figures 4.1, 4.3 and 4.4 the results of West Coast (WC) sample are omitted due to its high radium activity. The samples from the two mine dumps also have high radium activity concentration with Boksburg in the ranges of 92 - 1146 $Bq.kg^{-1}$ and Kloof in the ranges of 339 - 368 $Bq.kg^{-1}$. These high values from Boksburg and Kloof mine dump may be caused by the enhanced uranium contents at the mine dump due to mining processes. The lowest values for the radium activity concentration is for Centurion with 11 $Bq.kg^{-1}$, then Saldanha ranging from 15 - 34 $Bq.kg^{-1}$ and Paarl with ranges of 64 - 147 $Bq.kg^{-1}$. The granite rocks in Saldanha and Paarl do not have very high radium content, may be due to the uniform distribution of radium in the grains. The same is true for Centurion samples having low radium content. Soil samples that have high radium activity also have high radon concentrations as can be seen in the results.

The radon emanation coefficients were calculated using Equation 3.11. The emanation coefficient is the fraction of the radon atoms created that escapes into the pore space as discussed earlier. The radon emanation coefficient can have values between 0 and 1 (see chapter 1). The values of the radon emanation coefficient obtained is the highest in Centurion, Saldanha, Richards Bay Minerals, Paarl, Boksburg, Kloof and West Coast with values ranging from 0.812, 0.276 - 0.847, 0.765, 0.214 - 0.541, 0.063 - 0.313, 0.073 - 0.147 and 0.004, respectively. The West Coast sample has a high radium content but it does not emanate radon at all. The results obtained are comparable to the typical values of the radon emanation coefficient of 0.2 for soil samples as reported in UNSCEAR 2000. It has been observed that the emanation coefficient is unique for each soil sample and it varies for samples collected within the same location. The variations in the radon emanation coefficient may be caused by many factors, such as the differences in the radium activity concentration in the soil samples, the texture and grain size, and the permeability of the soil. The high values obtained in Centurion, Richards Bay Minerals, Saldanda and Paarl may suggest that the radium is distributed on the surface of the soil grains.

Low emanation coefficient obtained in Kloof and Boksburg may suggest that the radium is distributed uniformly in the soil grains. In Paarl the values of the radon emanation coefficient are typical values for soil in granitic areas. In Centurion only one soil sample was collected, which was very coarse, sandy soil, with high permeability hence the high emanation coefficient, although the emanation coefficient obtained may not be representative of the area and hence more samples should be analysed. The Kloof and Boksburg mine dump samples were comprised of processed rock with very fine particles like clay soil and hence the low permeability and porosity could have resulted in low emanation coefficient. The emanation coefficient of rocks and soils have values that range widely from up to about 0.05 and 0.70 with an average for soils between 0.20 and 0.30 [57]. Soils collected from the same parent rock at different regions or the same location have significantly different radon emanation coefficient such as the Saldanha and Paarl samples. Theoretically, ^{222}Rn concentration in the soil gas should be directly related to the uranium content of the mineral matter in the soil, however, the amount of radon that is produced in the soil is influenced by many of the factors mentioned above.

Figure 4.1, shows the variation of radium activity concentration in different locations. As can be seen in the figure, Boksburg mine dump samples have the highest radium activity concentration. Then followed by Kloof mine dump and Paarl. The Saldanha samples and Richards Bay Minerals have a lower radium activity concentration.

Figure 4.2, shows the radon concentration variation with increase in the masses of the sample. Boksburg has high radon concentration, followed by Kloof, Paarl and West Coast. The smallest radon concentration was obtained for soil samples from Saldanha, Centurion and Richards Bay Minerals. It can be observed from Figures 4.1 and 4.2 that an increase in the radium activity does not imply that there will be an increase in the radon concentration.
Figure 4.3 shows the increase in the created radon atoms with increase in radium activity concentration. As the radium activity increase, the fraction of radon atoms that escapes from the grains increases. The results from West Coast measurements are omitted in Figures 4.3-4.4 due to very high radium activity.
Figure 4.4, shows the decrease of the radon emanation coefficient as the radium activity increases in the different locations. This is the contrast to other studies that found that the radon emanation coefficient increases with an increase in the radium activity.

Figures 4.5 and 4.6 shows the graphs of radon concentration as the function of time. The best fit curves for the radon concentration have been fitted to the data points as shown in the figures. The solid line represents the best fit curve and the dots shows the measurement values and the line with marker is the average. The graphs shows a linear relationship of radon concentration with build up time. The measurements were conducted for a period of 48 hours. The radon concentration error bars are represented by the vertical lines. See appendix B for more graphs for the other locations.

The samples measured in this work were mostly from targeted areas where high values were expected. The samples in Paarl were collected in various areas on and close to the mountain, including a sample at one of the highest lying houses. The samples were collected at locations that were not close to each other, hence we do not necessarily expect the values to be the same. The same is true for the Boksburg samples, they were collected at a site where an old mine dump was situated. There is clearly some of the mine taillings still present at the site. Our sample locations were chosen after measuring with a dose meter.

The mine dump at kloof contains relatively uniform material from the mining operations, so the values are expected to be close to each other and that is what we found.

The West Coast sample was part of the thesis work of De Villiers 2011 [18]. This sample was collected at the Namakwa Sands mining company that mine heavy minerals on the West Coast of South Africa.

The Richards Bay Minerals sample was collected at the mining company. The mine produces Ilmenite which is a black mineral with submetallic to metallic luster.

Saldanha has a unique lithology incorporating two types of granite rocks, the I and the S types and also the Ignimbrite rocks. SP1 sample was taken from the Ignimbrite rocks area, SP2 sample was taken from the S-type granite rock area, SP3 was also taken from Ignimbrite rocks area at a different location and SP4 was taken from I-type granite rock area. From Table 4.2, the SP1 (Ignimbrite rock) has a high radium activity of 34 $Bq.kg^{-1}$. Followed by the SP3 (Ignimbrite rock) with radium activity of 30 $Bq.kg^{-1}$. SP4 (I-type granite) have radium

activity of 18 $Bq.kg^{-1}$ and SP2 (S-type granite) has the lowest radium activity of 15 $Bq.kg^{-1}$. These results shows that samples collected from Ignimbrite group rocks have a higher radium activity than the ones collected from the I and S type granite rocks. The radon emanation coefficient is the highest for SP4 (I-type granite) and lowest for SP1 (Ignimbrite) samples. SP2 (S-type) also have high emanation coefficient comparable to SP4 (I-type granite). These results indicate clearly that high radium activity samples do not necessarily emanate a lot of radon.

Chapter 5

Conclusion

5.0.1 A. Summary

In this chapter the results are reviewed and the future work is suggested.

Measurements were conducted to determine the radon emanation coefficient for soil samples in South Africa, for Kloof, Boksburg, Paarl, West Coast, Saldanha, Centurion and Richards Bay Minerals. The values of the emanation coefficient obtained in this study for sample mass of 0.256 kg ranges from, 0.073 - 0.146, 0.063 - 0.313, 0.214 - 0.541, 0.276 - 0.847, 0.812, 0.765 and 0.004, in Kloof, Boksburg, Paarl, Saldanha, Centurion, Richards Bay Minerals and West Coast, respectively. The radon emanation coefficient for sample mass of 0.512 kg are in the ranges from 0.092 - 0.108, 0.139 - 0.326, 0.171 - 0.572, 0.169 - 0.774, 0.188, 0.003, in Kloof, Boksburg, Paarl, Saldanha, Centurion, Richards Bay Minerals and West Coast, respectively. The radon emanation coefficient for the final sample mass to be investigated ranges from 0.089 - 0.113, 0.139 - 0.275, 0.245 - 0.373, 0.296 - 0.738, 0.686, 0.157, 0.003, in Kloof, Boksburg, Paarl, Saldanha, Centurion, Richards Bay Minerals and West Coast, respectively. The values of the emanation coefficient obtained agrees with the values from the UNSCEAR 2000 report of 0.01 - 0.8. The West Coast sample has a high radium content but it does not emanate much radon. More measurements should be conducted with more samples to get more information. The soil sample from Richards Bay Minerals and Centurion should be measured again in future studies, since only one sample was collected from each location. The radionuclide contents of radium and radon varies greatly for different lithologies.

The results indicate that none of the samples with high radium content have particularly high radon emanation coefficients. Hence none of these areas need particular attention during the National radon survey. The high emanation coefficient for some low radium areas such as Centurion and Saldanha indicate that these areas cannot be ignored. The radon emanation coefficient is important for evaluating the radon potential in the field, that can possibly escape to indoor structures. Radon concentration levels is the highest in Boksburg and lowest in Centurion. On the other hand, the radon emanation coefficient is the highest in Centurion and lowest in the West Coast. This study suggests that the houses in Centurion need to be measured for indoor radon levels as they are expected to be high. The houses in West Coast do not require immediate attention. However, it should be noted that a lot of factors need to be considered when determining the radon emanation coefficient such as moisture, temperature, grain size and permeability of the soil.

5.0.2 B. Outlook

Some suggestions for future work on radon emanation coefficient for soil measurements are:

- Radon concentration measurements should be conducted at the sampling site to compare with laboratory measurements.
- Chamber measurements should be conducted for more than 48 hours as the radon concentration increases as a function of time.
- Investigations should be made to evaluate the effect of grain size, moisture and porosity on the radon emanation coefficient.
- More samples should be studied to increase the accuracy in the radon emanation coefficient measurements.
- More full-energy peaks in the uranium decay series should be considered when measuring the activity of the soil to increase the accuracy in the activity concentration.

Appendix A

The one dimensional transport equation of radon across the Z-axis in a porous medium is given in equation A.1. A few approximations are assumed for resolving the equation analytically: Diffusion transport only (the pressure is constant in the chamber) and water content is neglected. Exhalation only occurs in the interface sample-air ($Z = 0$) [29].

$$\frac{\partial C}{\partial t} = D\frac{\partial^2 C}{\partial Z^2} - \lambda C + \frac{\lambda R \rho_b E}{n_e} \tag{A.1}$$

In this equation $\frac{\partial C}{\partial t}$ refers to the rate of change of the radon concentration, D$\frac{\partial^2 C}{\partial Z^2}$ refers to the loss of radon atoms by the process of diffusion, λC refers to the loss of radon atoms due to the radioactive decay and the last term $\frac{\lambda R \rho_b E}{n_e}$ refers to the creation rate of radon. The parameters in the last term are described below:
λ is the decay constant of radon ($2.1 \times 10^{-6} s^{-1}$),
R is the radium activity concentration,
ρ_b is the bulk density of the matrix,
E is the radon emanation coefficient and n_e is the partition corrected porosity.

At steady-state we have,

$$\frac{\partial C}{\partial t} = 0 \tag{A.2}$$

then we have,

$$D\frac{\partial^2 C}{\partial Z^2} - \lambda C + \frac{\lambda R \rho_b E}{n_e} = 0 \tag{A.3}$$

$$\frac{\partial^2 C}{\partial Z^2} - \frac{\lambda}{D} C + \frac{\lambda R \rho_b E}{D n_e} = 0 \tag{A.4}$$

$$\frac{\partial^2 C}{\partial Z^2} - \frac{\lambda}{D} C = -\frac{\lambda R \rho_b E}{D n_e} \tag{A.5}$$

Equation A.5 can be written in the form of a homogeneous second order differential equation as,

$$\frac{\partial^2 C}{\partial Z^2} - \frac{\lambda}{D} C = 0 \tag{A.6}$$

the general solution of this equation is

$$C(z) = Ae^{z/L} + Be^{-z/L} + \frac{R \rho_b E}{n_e} \tag{A.7}$$

where

$L = \sqrt{\frac{D}{\lambda}}$

and is the diffusion length of radon in a given matrix (i.e. soil in this study). A and B are unknown coefficients that can be found from the boundary conditions in a specific case. The constant term $\frac{R\rho_b E}{n_e}$ can be obtained as a particular solutions of Equation A.3. In this study the sample thickness was made to be less than the diffusion length of radon in soil. Therefore the radon concentration created in the pore spaces can be assumed to be very close to the concentration entering the air in the chamber volume.The radon measurement can be simplified to a set-up where we have soil containing radium with a large air volume above as schematically indicated in Figure A.1.

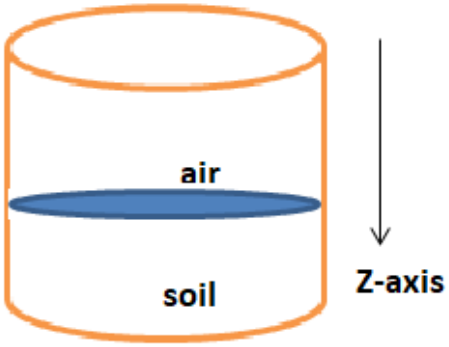

Figure A.1: Schematic of soil containing radon in the chamber.

If we apply this result to the simplified, one dimensional situation with a Z-axis running downward and Z=0 at the air/soil interface, we find that the constant A=0, since the concentration must be finite for large z (a more accurate result is possible by taking the finite depth of soil into account, but the result is essentially the same). At Z=0, the value in the air is much less than in the soil and can be approximated as 0. This implies:

$$B \approx -\frac{R\rho_b E}{n_e} \tag{A.8}$$

Hence $C(z) = \frac{\lambda R\rho_b E}{n_e}(1 - e^{-z/L})$

Appendix B

Figures B.1-B.14 shows the radon concentration graphs as a function of time for different locations. The model fit (Equation 3.14) the results well for some graphs (see Figures B.1 and B.13) where the Chi-squared values are close to one and for others graphs it fails (see Figures B.2-B.14), where the Chi-squared values are close to zero.

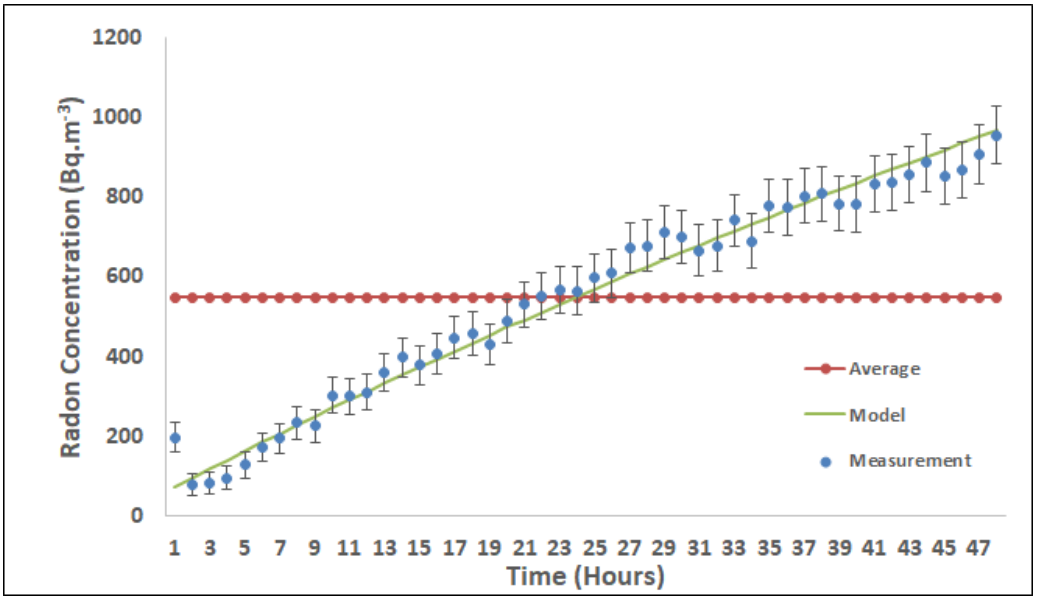

Figure B.1: A graph showing the radon concentration as a function of time for Boksburg sample (BP1).

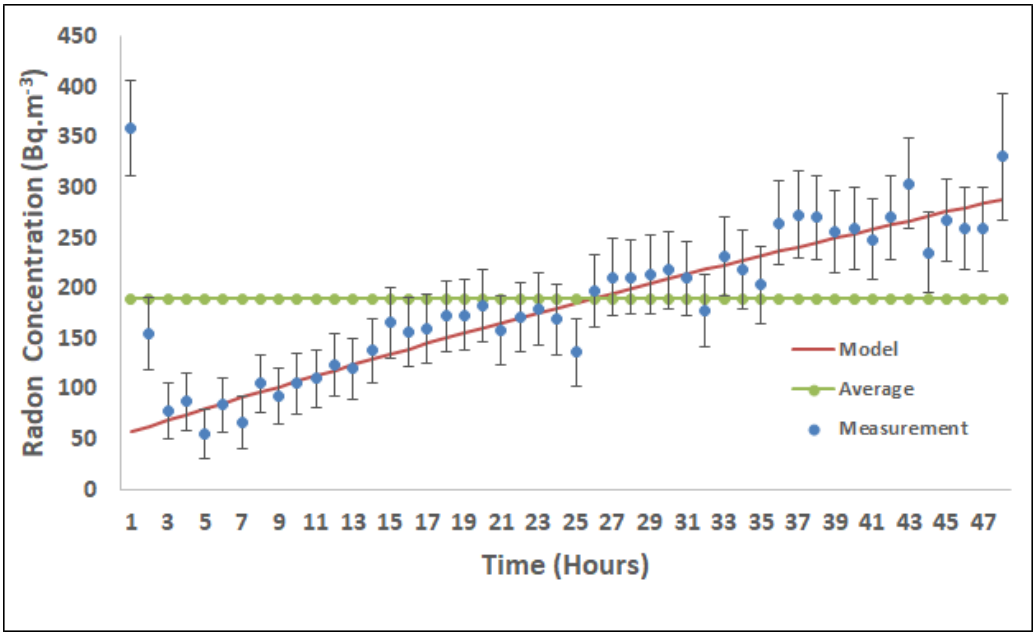

Figure B.2: A graph showing the radon concentration as a function of time for Boksburg sample (BP2).

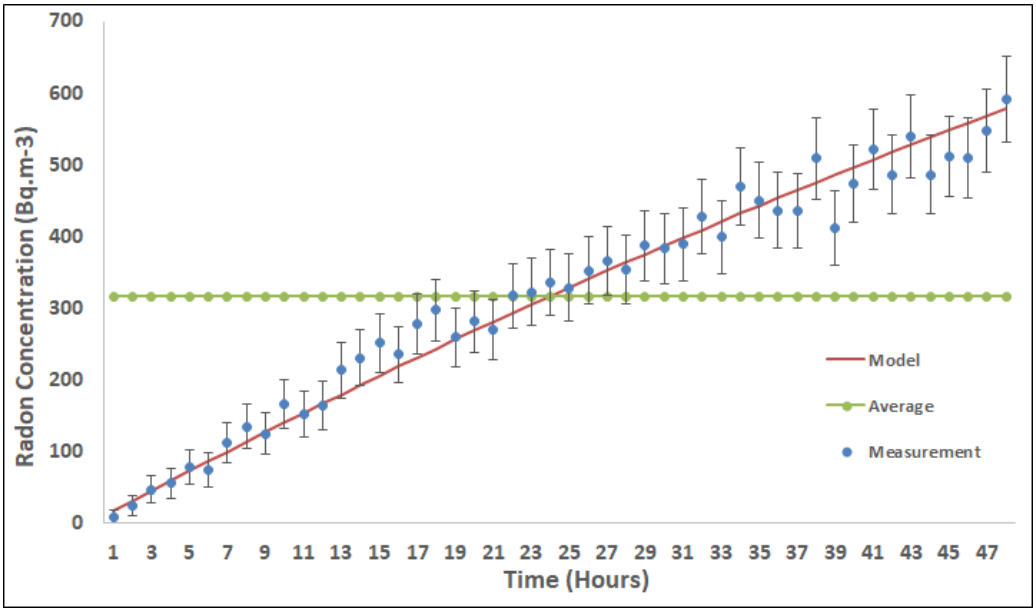

Figure B.3: A graph showing the radon concentration as a function of time for Boksburg sample (BP3).

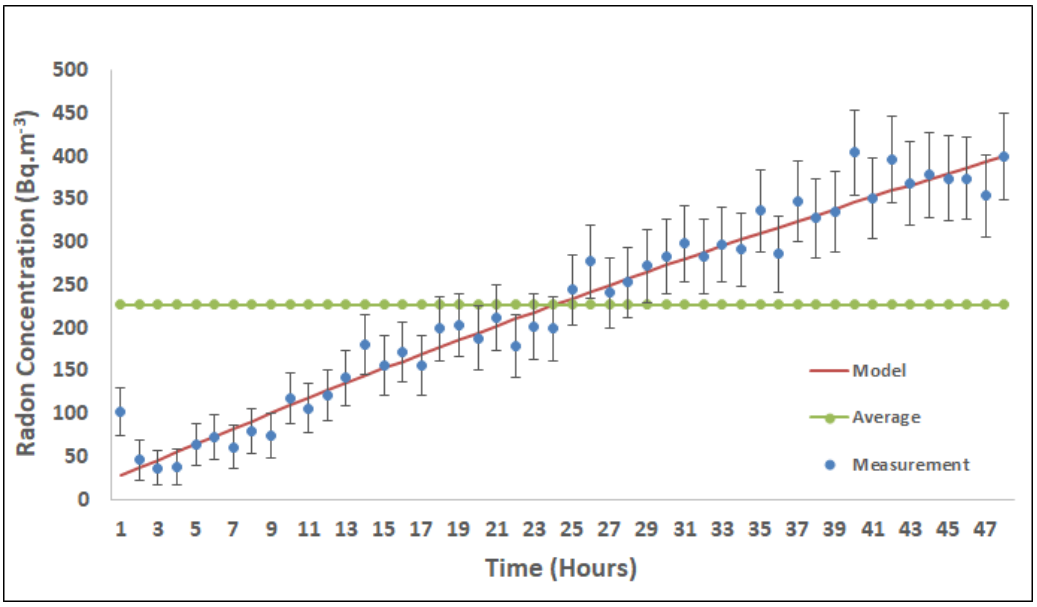

Figure B.4: A graph showing the radon concentration as a function of time for Kloof sample (KS51).

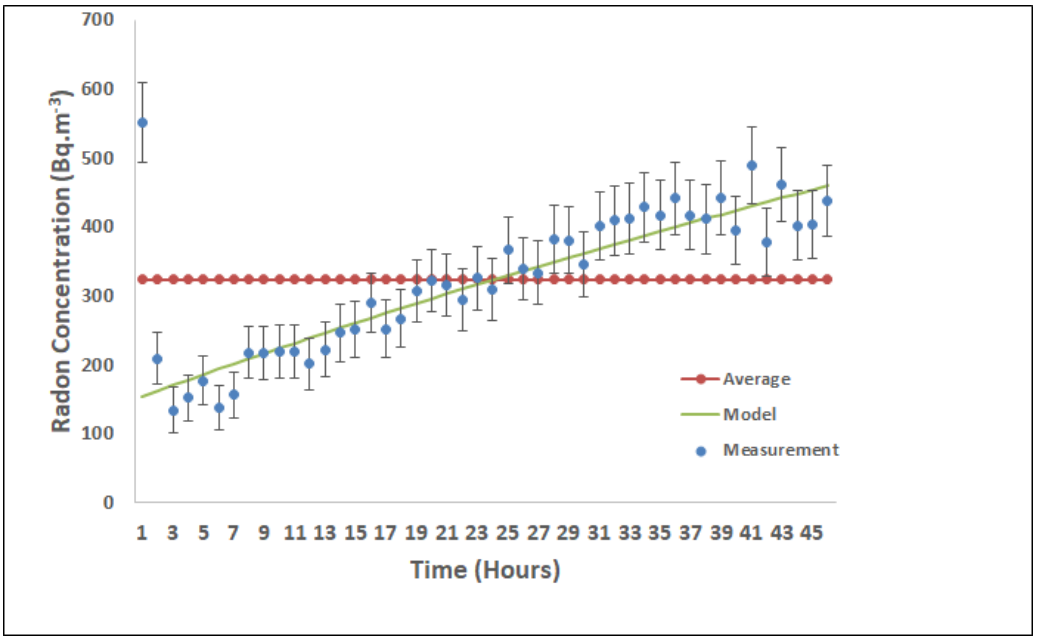

Figure B.5: A graph showing the radon concentration as a function of time for Kloof sample (KS41B).

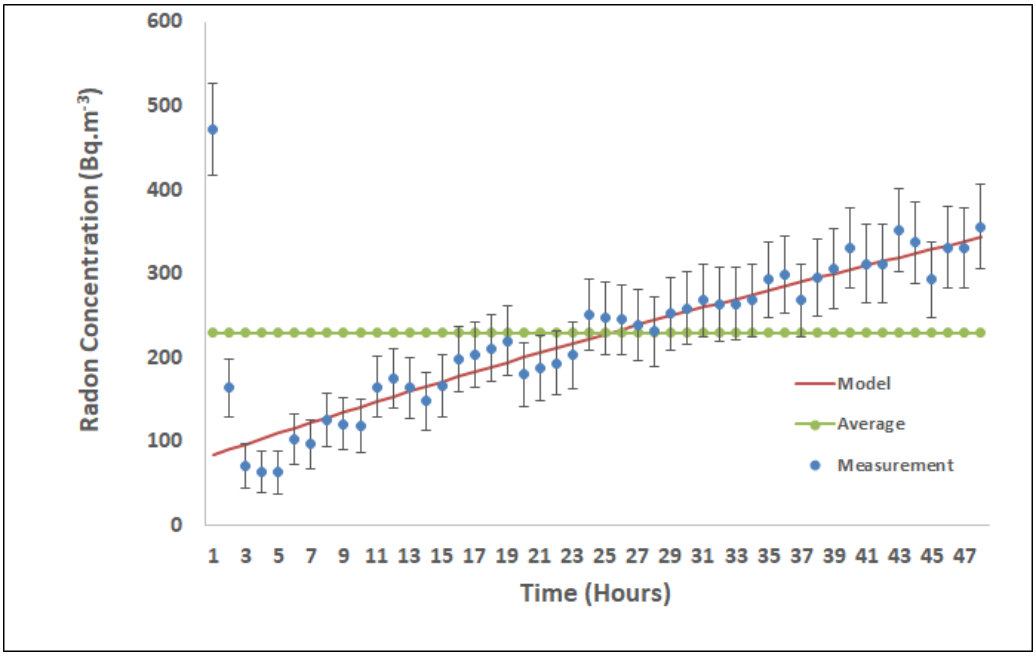

Figure B.6: A graph showing the radon concentration as a function of time for Paarl sample (PP5).

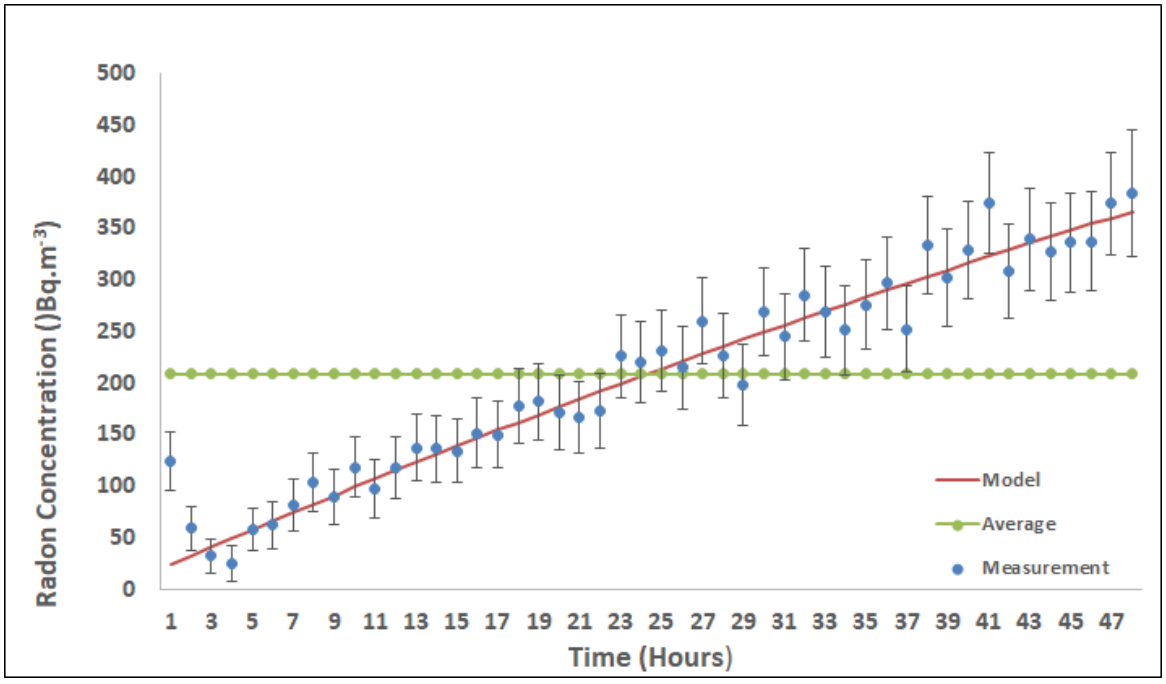

Figure B.7: A graph showing the radon concentration as a function of time for Paarl sample (PP6).

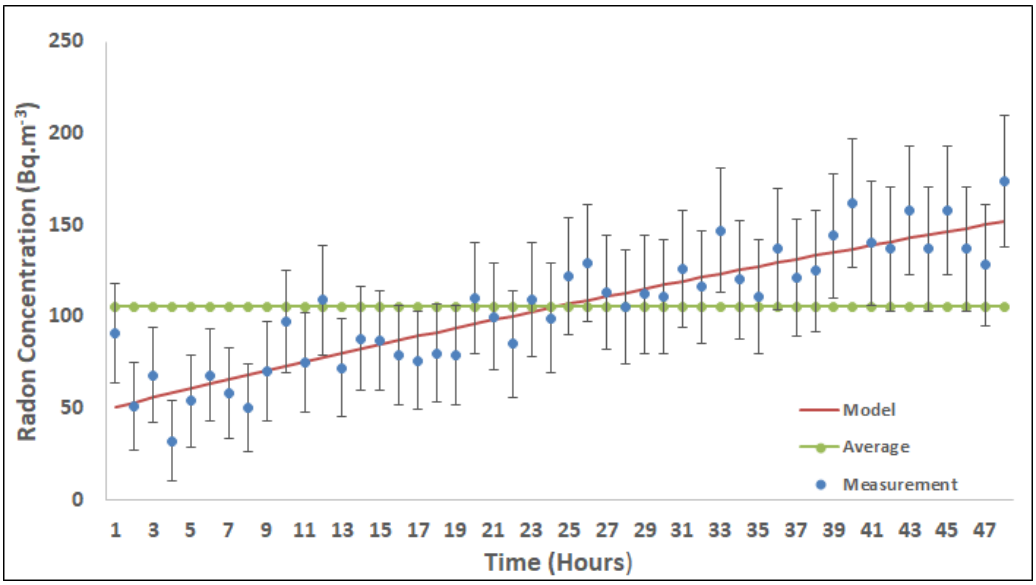

Figure B.8: A graph showing the radon concentration as a function of time for Saldanha sample (SP1).

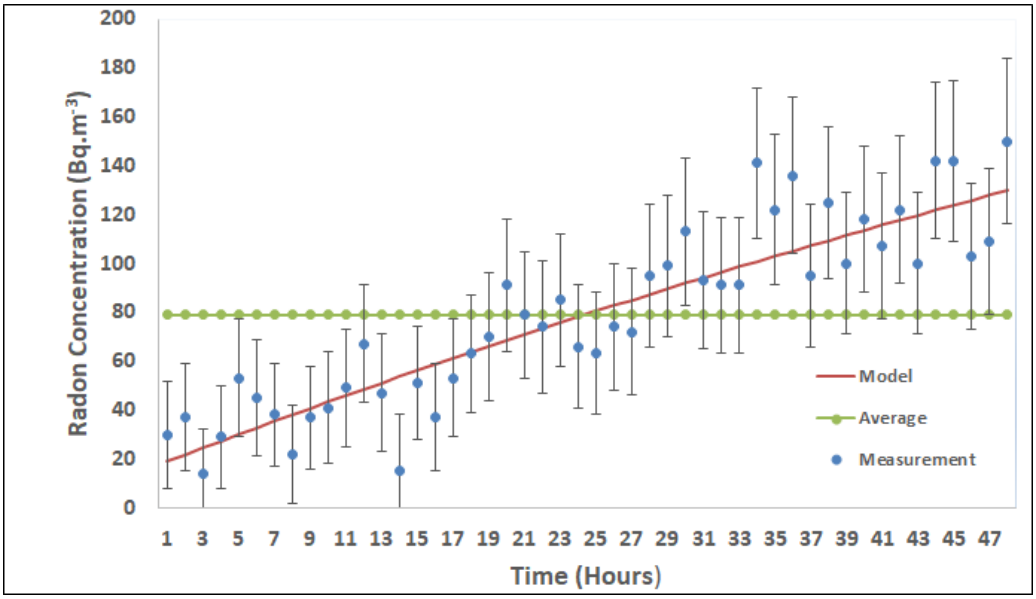

Figure B.9: A graph showing the radon concentration as a function of time for Saldanha sample (SP2).

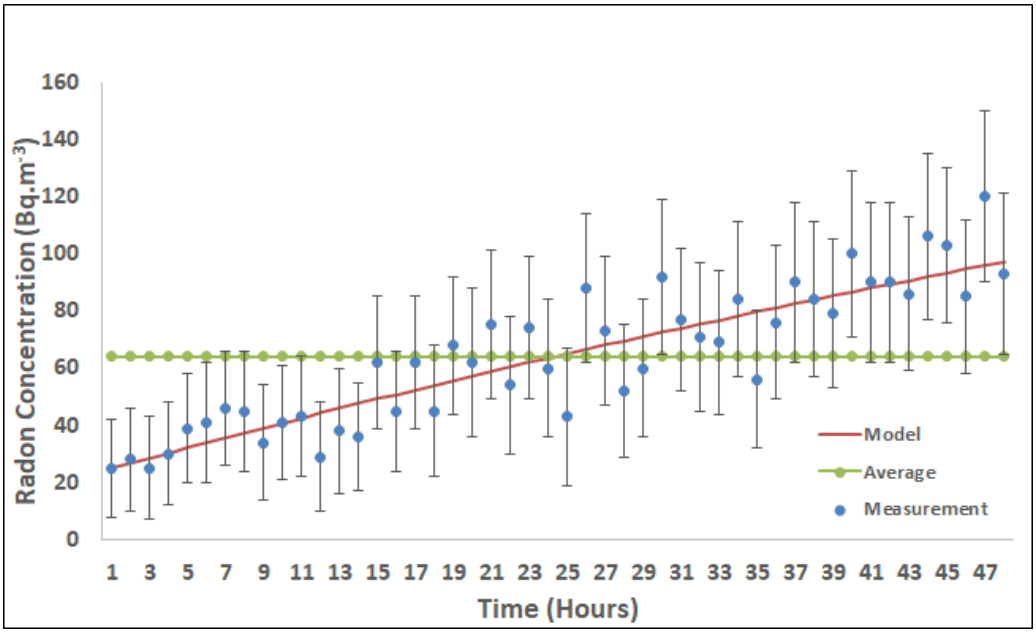

Figure B.10: A graph showing the radon concentration as a function of time for Saldanha sample (SP3).

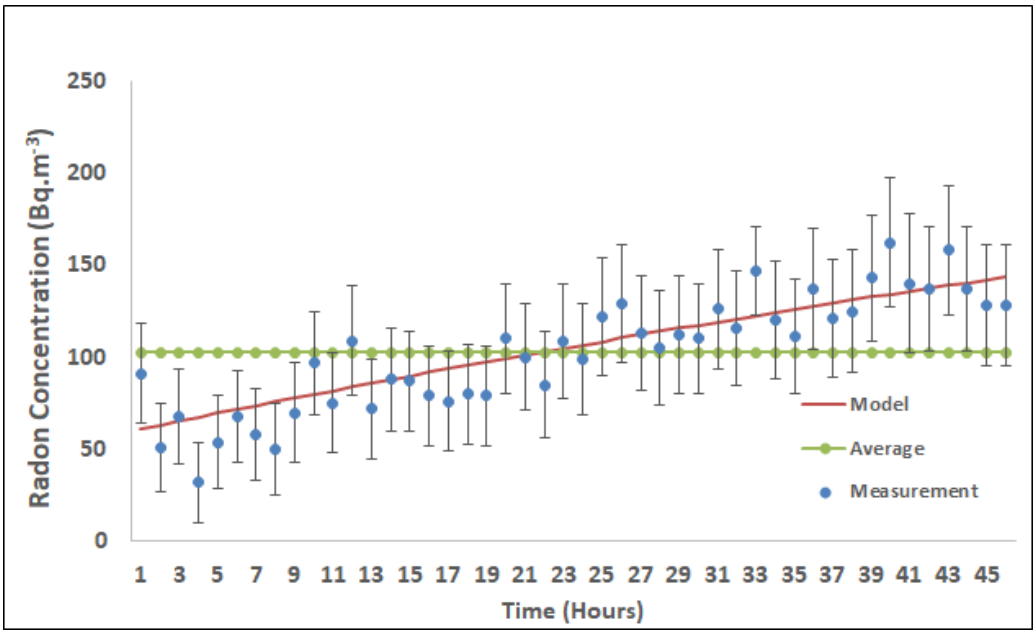

Figure B.11: A graph showing the radon concentration as a function of time for Saldanha sample (SP4).

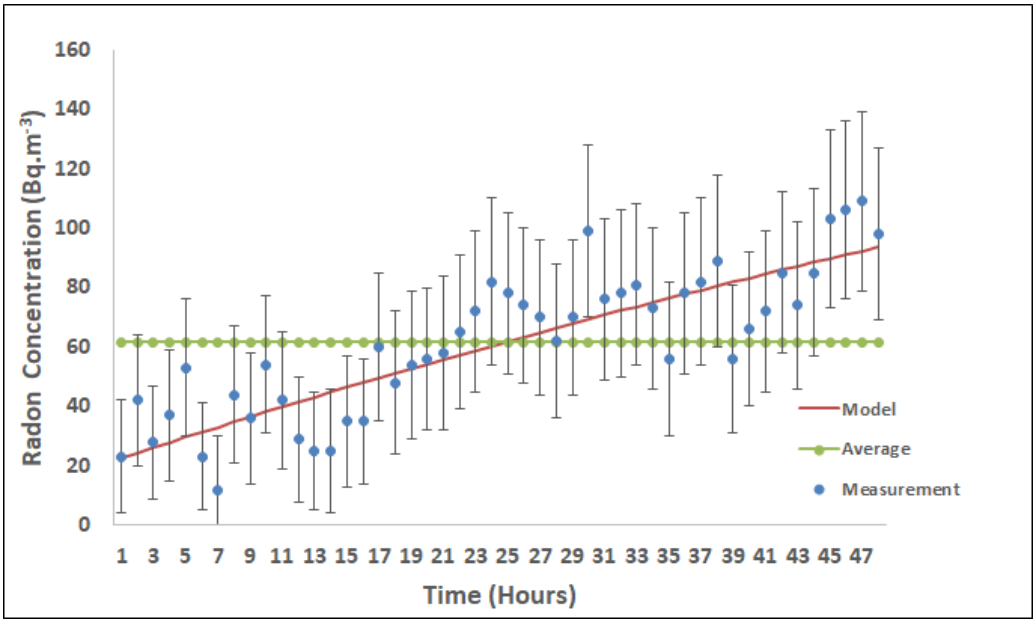

Figure B.12: A graph showing the radon concentration as a function of time for Centurion sample (CP1).

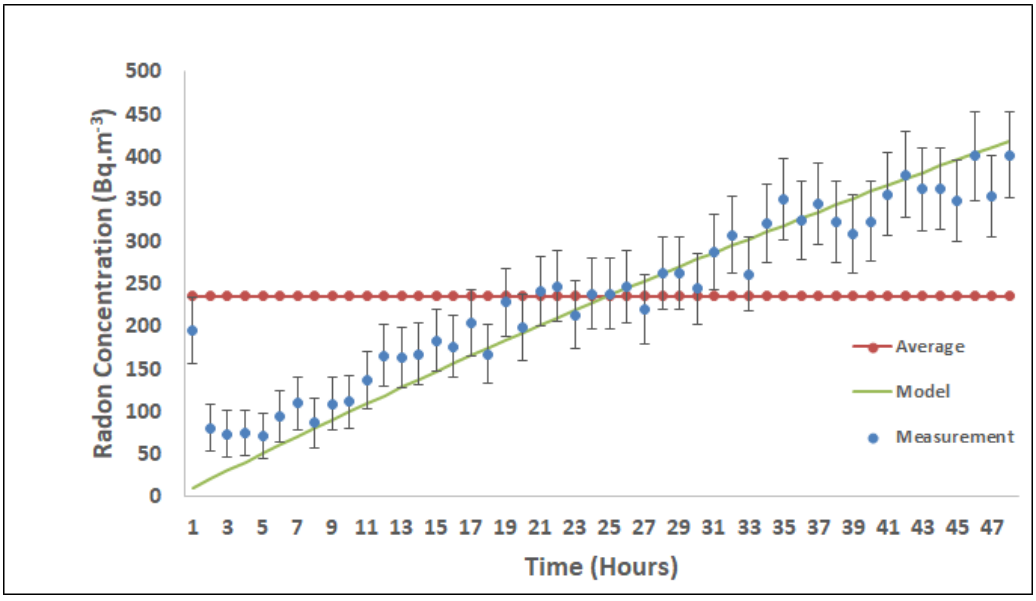

Figure B.13: A graph showing the radon concentration as a function of time for West Coast sample (WC).

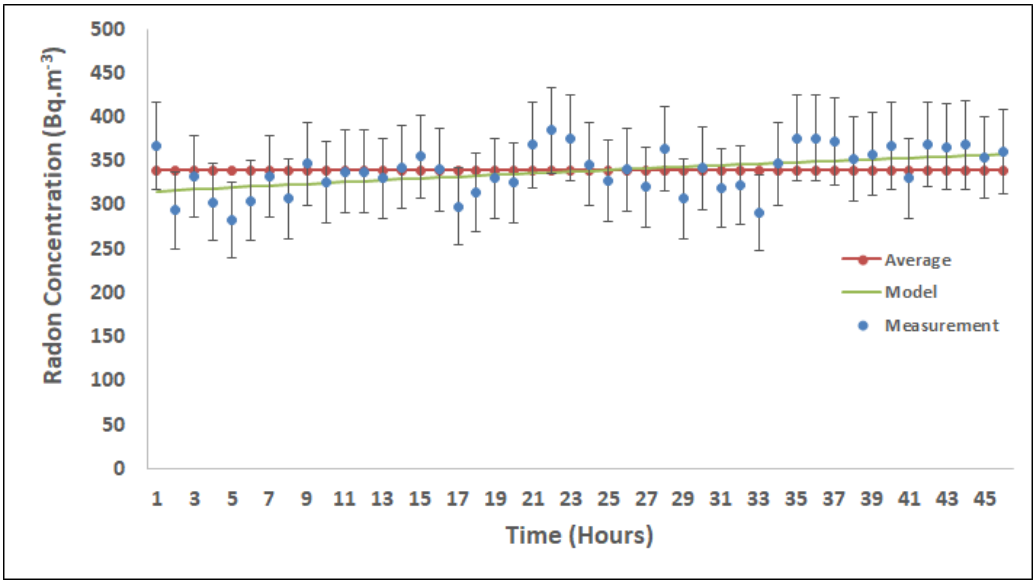

Figure B.14: A graph showing the radon concentration as a function of time for Richards Bay Minerals sample (RBM)

Appendix C

The uncertainties in the activity concentration were obtained using the following equation:

$$\frac{U_c(A)}{A} = \sqrt{\frac{U(m)^2}{m} + \frac{U(C_{net})^2}{C_{net}} + \frac{U(Br)^2}{Br} + \frac{U(\epsilon)^2}{\epsilon}} \tag{C.1}$$

The parameters in equation C.1 are already defined in Chapter 3 [16].

Table C.1 shows the different sources that contribute to the uncertainties in the activity measurements.

Table C.1: Sources of uncertainties in the activity concentration [16].

Uncertainty Source	Symbol used	Uncertainty range(%)	Typical uncertainty value (%)
Counting	C_{net}	0.1-20	5
Emission probability	Br	0.1-11	< 2
Detector efficiency	ϵ	1-5	2
Sample mass	m	0.01-1	< 0.5

Bibliography

[1] KM Abumurad et al. "Determination of radon soil concentration levels in the Governorate of Irbid, Jordan". In: *Radiation Measurements* 28.1-6 (1997), pp. 585–588.

[2] Julio C Aguiar, Eduardo Galiano, and Jorge Fernandez. "Peak efficiency calibration for attenuation corrected cylindrical sources in gamma ray spectrometry by the use of a point source". In: *Applied Radiation and Isotopes* 64.12 (2006), pp. 1643–1647.

[3] Mohammed D Alenezy. "Radon concentrations measurement in Aljouf, Saudi Arabia using active detecting method". In: *Natural Science* 6.11 (2014), p. 886.

[4] J Argyriades et al. "Measurement of the background in the NEMO 3 double beta decay experiment". In: *Nuclear Instruments and Methods in Physics Research Section A: Accelerators, Spectrometers, Detectors and Associated Equipment* 606.3 (2009), pp. 449–465.

[5] C Baixeras et al. "Radon emanation from soil samples". In: *Radiation Measurements* 34.1-6 (2001), pp. 441–443.

[6] Rémi Barillon, Ahmet Özgümüs, and Alain Chambaudet. "Direct recoil radon emanation from crystalline phases. Influence of moisture content". In: *Geochimica et Cosmochimica Acta* 69.11 (2005), pp. 2735–2744.

[7] Tomislav Bituh. "The Environmental Behaviour of Radium: Revised Edition (Technical Reports Series No. 476)". In: *Archives of Industrial Hygiene and Toxicology* 65.2 (2014), A20–A20.

[8] Peter Bossew. "The radon emanation power of building materials, soils and rocks". In: *Applied Radiation and Isotopes* 59.5-6 (2003), pp. 389–392.

[9] D Breitner et al. "Effect of moisture content on emanation at different grain size fractions–A pilot study on granitic esker sand sample". In: *Journal of Environmental Radioactivity* 101.11 (2010), pp. 1002–1006.

[10] KM Chang. "Analytical Methodology for the Determination of Radium Isotopes in Environmental Samples". In: *International Atomic Energy Agency, Vienna* (2010).

[11] Christopher YH Chao et al. "Determination of radon emanation and back diffusion characteristics of building materials in small chamber tests". In: *Building and Environment* 32.4 (1997), pp. 355–362.

[12] P Chiozzi et al. "Laboratory application of NaI (Tl) γ-ray spectrometry to studies of natural radioactivity in geophysics". In: *Applied Radiation and Isotopes* 53.1-2 (2000), pp. 127–132.

[13] Gregory Choppin, Jan-Olov Liljenzin, and Jan Rydberg. Radiochemistry and nuclear chemistry. *Butterworth-Heinemann*, (2002).

[14] Constantin Cosma et al. "Soil and building material as main sources of indoor radon in Băiţa-Ştei radon prone area (Romania)". In: *Journal of Environmental Radioactivity* 116 (2013), pp. 174–179.

[15] National Research Council et al. Health effects of exposure to radon: BEIR VI. Vol. 6. *National Academies Press*, (1999).

[16] Lloyd A Currie. "Quantifying Uncertainty in Nuclear Analytical Measurements". Tech. rep. (2004).

[17] Salvatore De Martino, Carlo Sabbarese, and Giulia Monetti. "Radon emanation and exhalation rates from soils measured with an electrostatic collector". In: *Applied Radiation and Isotopes* 49.4 (1998), pp. 407–413.

[18] Dawid De Villiers. "Characterisation of heavy mineral sands and soils by radiometry and its use in mineral benefication and agriculture". PhD thesis. Stellenbosch University, (2011).

[19] Saeed A Durrani et al. Radon measurements by etched track detectors: applications in radiation protection, earth sciences and the environment. *World Scientific*, (1997).

[20] United Nations. Scientific Committee on the Effects of Atomic Radiation. Effects of ionizing radiation: UNSCEAR 2006 report to the general assembly, with scientific annexes. Vol. 2. *United nations publications*, (2008).

[21] Alwyn Petrus Geyser. "The influence of geographic factors on the distribution of natural radionuclides". MSc thesis. Stellenbosch University, (2017).

[22] Daniel J Greeman and Arthur W Rose. "Factors controlling the emanation of radon and thoron in soils of the eastern USA". In: *Chemical Geology* 129.1-2 (1996), pp. 1–14.

[23] Nabil M Hassan et al. "Radon migration process and its influence factors; review". In: *Japanese Journal of Health Physics* 44.2 (2009), pp. 218–231.

[24] Robert Hayes and Hung Cheng Chiou. "Preliminary evaluation of real time false CAM alarm prediction through continuous radon monitoring". In: *Health Physics* 84.5 (2003), S89–S92.

[25] PHGM Hendriks, J Limburg, and RJ De Meijer. "Full-spectrum analysis of natural γ-ray spectra". In: *Journal of Environmental Radioactivity* 53.3 (2001), pp. 365–380.

[26] M Herranz et al. "Radon fixation for determination of ^{224}Ra, ^{226}Ra and ^{228}Ra via gamma-ray spectrometry". In: *Radiation Measurements* 41.4 (2006), pp. 486–491.

[27] K Holy et al. "Radon emanation coefficients in sandy soils". In: (1998).

[28] John G Ingersoll. "A survey of radionuclide contents and radon emanation rates in building materials used in the US". In: *Health Physics* 45.2 (1983), pp. 363–368.

[29] Yuu Ishimori et al. Measurement and calculation of radon releases from NORM residues. *IAEA*, (2013).

[30] Dadong Iskandar, Hiromi Yamazawa, and Takao Iida. "Quantification of the dependency of radon emanation power on soil temperature". In: *Applied Radiation and Isotopes* 60.6 (2004), pp. 971–973.

[31] Paweł Jodłowski. "Self-absorption correction in gamma-ray spectrometry of environmental samples-an overview of methods and correction values obtained for the selected geometries". In: *Nukleonika* 51 (2006), pp. 21–25.

[32] Bernd Kahn, Robert Rosson, and Joel Cantrell. "Analysis of ^{228}Ra and ^{226}Ra in public water supplies by a gamma-ray spectrometer." In: *Health Physics* 59.1 (1990), pp. 125–131.

[33] Glenn F Knoll. Radiation Detection and Measurement. *John Wiley & Sons*, (2010).

[34] K Kovler et al. "Radon exhalation of cementitious materials made with coal fly ash: Part 1–scientific background and testing of the cement and fly ash emanation". In: *Journal of Environmental Radioactivity* 82.3 (2005), pp. 321–334.

[35] Jong-Mi Lee and Guebuem Kim. "A simple and rapid method for analyzing radon in coastal and ground waters using a radon-in-air monitor". In: *Journal of Environmental Radioactivity* 89.3 (2006), pp. 219–228.

[36] R Lindsay, RT Newman, and WJ Speelman. "A study of airborne radon levels in Paarl houses (South Africa) and associated source terms, using electret ion chambers and gamma-ray spectrometry". In: *Applied Radiation and Isotopes* 66.11 (2008), pp. 1611–1614.

[37] R.H Morse Associates Ltd. The Lucas cell:the standard for radon, radium and thoron. (1968). URL: `http://www.finderschoice.com/radon/lucasCell.php` (visited on 12/04/2019).

[38] Jay H Lubin et al. "Radon-exposed underground miners and inverse dose-rate (protraction enhancement) effects". In: *Health Physics* 69.4 (1995), pp. 494–500.

[39] Lennart Malmqvist, Mats Isaksson, and Krister Kristiansson. "Radon migration through soil and bedrock". In: *Geoexploration* 26.2 (1989), pp. 135–144.

[40] Ramudzuli Fijiant Manavhela. "In-situ measurements of radon concentrations in soil gas at a site on the Cape Flats". MSc thesis. University of the Western Cape, (2007).

[41] Rad7 User Manual. *Durridge co.* (2000).

[42] L Morawska and Colin R Phillips. "Dependence of the radon emanation coefficient on radium distribution and internal structure of the material". In: *Geochimica et Cosmochimica Acta* 57.8 (1993), pp. 1783–1797.

[43] Mashinga Johannes Mvelase. "Radon escape from water". MSc thesis. University of the Western Cape, (2010).

[44] William W Nazaroff. "Radon transport from soil to air". In: *Reviews of geophysics* 30.2 (1992), pp. 137–160.

[45] G Nelson and D Reilly. "Gamma-ray interactions with matter". In: *Passive nondestructive analysis of nuclear materials* (1991), pp. 27–42.

[46] Ahmad E Nevissi and David Bodansky. "Radon sources and levels in the outside environment". In: *Indoor radon and its hazards*. (1987).

[47] Joash Nyakondo Ongori. "In-situ measurements and calculation of radon gas concentration and exhalation from a tailings mine dump". PhD thesis. University of the Western Cape, (2013).

[48] World Health Organization et al. WHO handbook on indoor radon: a public health perspective. *World Health Organization*, (2009).

[49] Pravin Parekh et al. "Non-destructive determination of ^{224}Ra, ^{226}Ra and ^{228}Ra concentrations in drinking water by gamma spectroscopy". In: *Health Physics* 85.5 (2003), pp. 613–620.

[50] RC Ramola et al. "The use of radon as an earthquake precursor." In: *INT. J. RADIAT. APPLIC. INSTRUM., PART E.* 4.2 (1990), pp. 275–287.

[51] Sophie Rihs and Michel Condomines. "An improved method for Ra isotope (^{226}Ra, ^{228}Ra, ^{224}Ra) measurements by gamma spectrometry in natural waters: application to CO_2-rich thermal waters from the French Massif Central". In: *Chemical Geology* 182.2-4 (2002), pp. 409–421.

[52] Venn C Rogers and Kirk K Nielson. "Radon emanation and transport in porous media". In: *Proceedings of the 1988 EPA Symposium on Radon and Radon Reduction Methods*. Vol. 1. (1988), pp. 45–58.

[53] Patitapaban Sahu et al. "Radon emanation from low-grade uranium ore". In: *Journal of Environmental Radioactivity* 126 (2013), pp. 104–114.

[54] Akihiro Sakoda et al. “First model of the effect of grain size on radon emanation”. In: *Applied Radiation and Isotopes* 68.6 (2010), pp. 1169–1172.

[55] Gerald L Schroeder, Hobart W Kraner, and Robley D Evans. “Diffusion of radon in several naturally occurring soil types”. In: *Journal of Geophysical Research* 70.2 (1965), pp. 471–474.

[56] M Schubert et al. “In situ determination of radon in surface water bodies by means of a hydrophobic membrane tubing”. In: *Radiation Measurements* 43.1 (2008), pp. 111–120.

[57] R Randall Schumann. “The radon emanation coefficient: an important tool for geologic radon potential estimations”. In: *Proceedings of the 1993 International Radon Conference, Sept.* (1993), pp. 20–22.

[58] TM Semkow et al. “Low-background gamma spectrometry for environmental radioactivity”. In: *Applied Radiation and Isotopes* 57.2 (2002), pp. 213–223.

[59] Prem V Sharma. Environmental and engineering geophysics. *Cambridge University Press*, (1997).

[60] Y Shiroma et al. “Estimation of radon emanation coefficient for representative soils in Okinawa, Japan”. In: *Radiation protection dosimetry* 167.1-3 (2015), pp. 147–150.

[61] J Søgaard-Hansen and Anders Damkjaer. “Determining ^{222}Rn diffusion lengths in soils and sediments.” In: *Health physics* 53.5 (1987), pp. 455–459.

[62] János Somlai et al. “Radon concentration in houses over a closed Hungarian uranium mine”. In: *Science of the total Environment* 367.2-3 (2006), pp. 653–665.

[63] Wilcot John Speelman. “Modelling and measurement of radon diffusion through soil for application on mine tailings dam”. MSc thesis. University of the Western Cape, (2004).

[64] Thomas Stieglitz. “Submarine groundwater discharge into the near-shore zone of the Great Barrier Reef, Australia”. In: *Marine Pollution Bulletin* 51.1-4 (2005), pp. 51–59.

[65] Allan Bain Tanner. Radon migration in the ground: a supplementary review. Tech. rep. (1980).

[66] Mirion Technologies. Types of Ionizing Radiation. (2015). URL: `http://www.mirion.com/learning-center/radiation-safety-basics/types-of-ionizing-radiation` (visited on 11/20/2019).

[67] A UNSCEAR. United Nations Scientific Committee on the Effects of Atomic Radiation. (2000).

[68] M Jurado Vargas et al. “Monte Carlo simulation of the self-absorption corrections for natural samples in gamma-ray spectrometry”. In: *Applied Radiation and Isotopes* 57.6 (2002), pp. 893–898.

[69] Hiroshi Wakita et al. “Radon anomaly: a possible precursor of the 1978 Izu-Oshima-Kinkai earthquake”. In: *Science* 207.4433 (1980), pp. 882–883.

[70] Hannelore Waska et al. “An efficient and simple method for measuring ^{226}Ra using the scintillation cell in a delayed coincidence counting system (RaDeCC)”. In: *Journal of Environmental Radioactivity* 99.12 (2008), pp. 1859–1862.

[71] Y Wu et al. “Radon concentration: A tool for assessing the fracture network at Guanyinyan study area, China”. In: *Water SA* 29.1 (2003), pp. 49–53.

[72] James F Ziegler and Jochen P Biersack. “The stopping and range of ions in matter”. In: *Treatise on Heavy-Ion Science*. Springer, (1985), pp. 93–129.